ELSEVIER

Applied Catalysis A: General 181 (1999) 355–398

APPLIED CATALYSIS A: GENERAL

Disproportionation and transalkylation of alkylbenzenes over zeolite catalysts

Tseng-Chang Tsai[a], Shang-Bin Liu[b], Ikai Wang[c,*]

[a]*Refining and Manufacturing Research Center, Chinese Petroleum Corporation, Chiayi 600, Taiwan*
[b]*Institute of Atomic and Molecular Sciences, Academia Sinica, PO Box 23-166, Taipei 106, Taiwan*
[c]*Department of Chemical Engineering, National Tsing-Hua University, Hsinchu 300, Taiwan*

Received 13 June 1998; received in revised form 3 October 1998; accepted 5 November 1998

Abstract

Disproportionation and transalkylation are important processes for the interconversion of mono-, di-, and tri-alkylbenzenes. In this review, we discuss the recent advances in process technology with special focus on improvements of *para*-isomer selectivity and catalyst stability. Extensive patent search and discussion on technology development are presented. The key criteria for process development are identified. The working principles of *para*-isomer selectivity improvements involve the reduction of diffusivity and the inactivation of external surface. In conjunction with the fundamental research, various practical modification aspects particularly the pre-coking and the silica deposition techniques, are extensively reviewed. The impact of *para*-isomer selective technology on process economics and product recovery strategy is discussed. Furthermore, perspective trends in related research and development are provided.

Keywords: Disproportionation; Transalkylation; Alkylbenzenes; Zeolites; Diffusivity

1. Introduction

Aromatics have a wide variety of applications in the petrochemical and chemical industries. They are an important raw material for many intermediates of commodity petrochemicals and valuable fine chemicals, such as monomers for polyesters, engineering plastics, intermediates for detergents, pharmaceuticals, agricultural-products and explosives [1]. Among them, benzene, toluene and xylenes (BTX) are the three basic materials for most intermediates of aromatic derivatives (Fig. 1) [2].

Dialkylbenzenes, a subcategory of aromatics, include xylenes, diethylbenzene (DEB) and dipropylbenzene (DPB), all of which may be derivable to valuable performance chemicals. For example, xylenes are the key raw materials for polyesters, plasticizers and engineering plastics [3], *p*-DEB is a high-valued desorbent used in *p*-xylene adsorptive separation process [4], whereas increasing applications of diisopropylbenzene (DIPB) have been found, ranging from photo-developers, antioxidants to engineering plastics [5]. Process development in aromatic interconversion is therefore an important research task with great industrial demands.

There are many driving forces for the development of a new process. In addition to the economically

*Corresponding author.

0926-860X/99/$ – see front matter
PII: S0926-860X(98)00396-2

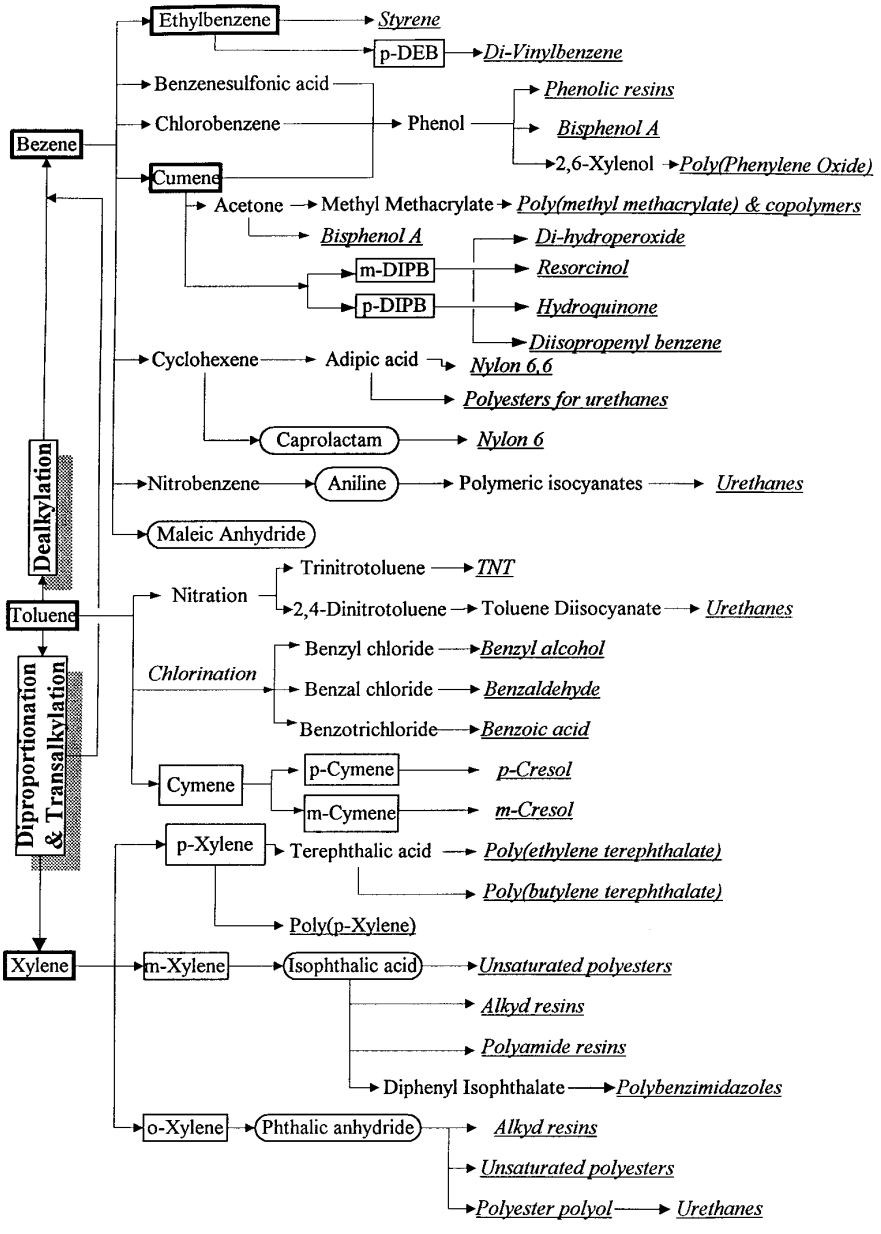

Fig. 1. Derivatives of benzene, toluene and xylene; from refs. [1,2].

relevant variables such as market demand, feedstock availability and cost, and operating cost, legislative aspects such as environmental laws, and new reformulated gasoline specifications, etc., also come into play.

In response to the worldwide environmental awareness, there are active programs to search for clean processes. Solid acid catalysts have long been demonstrated as the keys to the success of the historical efforts. Tanabe et al. [6] comprehensively discussed acid catalyst properties in his well-known review in solid acids and bases. Aromatics alkylation was one typical example of the use of solid acid catalysts in the development of environmentally sound processes.

Zeolites were used to replace the traditional Friedel–Craft catalysts, making the process cleaner, less corrosive and more economic competitive. By using Friedel–Craft catalysts, solid and liquid wastes in ethylbenzene (EB) production of 390 000 tons/year were 500 and 800 tons/year, respectively. By using ZSM-5 catalyst, the wastes were significantly reduced to 35 and 264 tons/year, respectively [7].

The 1990 Clean Air Act (CAA) had re-defined the gasoline specifications to enforce the so-called "reformulated gasoline" (RFG) act [8]. The initial stage of the enforcement applied the Simple Model regulation, by which the maximum benzene content in gasoline is limited to less than 1 vol% [9,10]. In a later stage, a Complex Model regulation will be applied, by which the maximum content of total aromatics is likely to be limited to as low as 25 vol%. As a result, many international projects have been developed to modify refinery structures in order to meet the challenge. The modifications involved switching the application of aromatics from gasoline to petrochemicals, especially to benzene and xylenes. The composition restrictions imposed on the "reformulated gasoline" therefore not only have significant impact on gasoline composition, but also on the economics of aromatics production processes.

The processes of catalytic reforming and naphtha pyrolysis are the main sources of BTX production. The product yields of those processes are normally controlled by thermodynamics and hence result in a substantial mismatch between the supply and the actual market demands. As shown in Fig. 2, the world-wide production capacity ratio for B:T:X obtained from the two above mentioned processes is 32:36:32 [11], and varies with regional locations. This contrasts to their market demands in petrochemical industry (without accounting for the demand in gasoline pool) of 55:11:34 [12–16]. In other words, toluene which has the lowest market demand is always in surplus from the production of reformate and pyrolysis gasoline, whereas benzene and xylenes are in strong demand with the average annual growth rates of around 10% [16–18], as shown in Fig. 3. As a result of demand and supply, the price for toluene is always lower than the other aromatics. For example, the historical BTX market price in Europe is presented in Fig. 4. The conversion of dispensable toluene into the more valuable aromatics therefore has an economic incentive. A serious discrepancy between production and market demand was also found for most dialkylbenzene isomers, among which the *para*-isomer apparently has the greatest market demand.

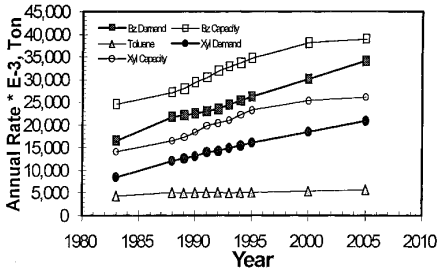

Fig. 3. Worldwide BTX market growth curves.

In response to market situation and legislation changes, the main areas of new aromatics process innovations were:

1. conversion of surplus toluene,

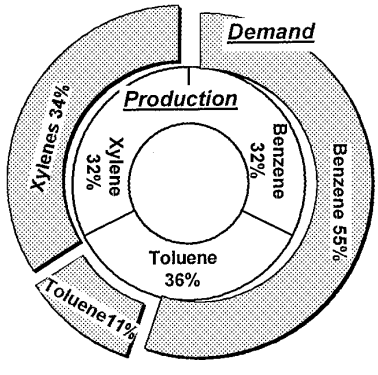

Fig. 2. Comparison of worldwide BTX distribution patterns of production and market demand.

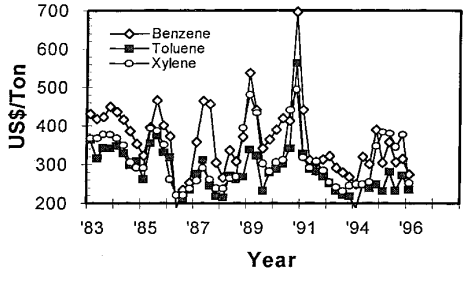

Fig. 4. Historical BTX price in Europe market.

2. upgrading of heavy aromatics, which are benzene and xylene (B & X) oriented,
3. selective production of *para*-dialkylbenzene isomer against thermodynamic equilibrium, such as *p*-xylene and *p*-DEB, and
4. production of dialkylbenzenes with carbon number of alkyl group larger than 3.

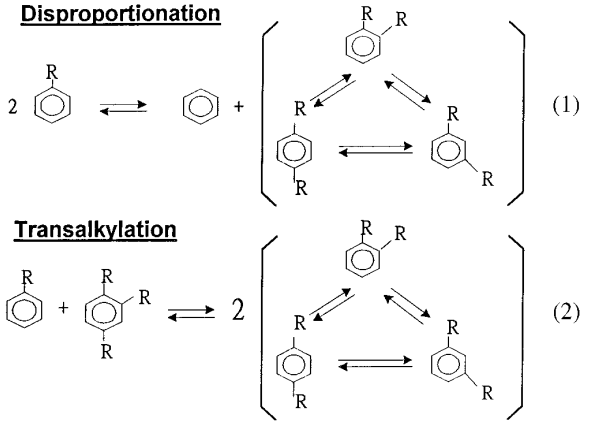

(1)

(2)

Disproportionation and transalkylation are the two major practical processes for the interconversion of aromatics, especially for the production of dialkylbenzenes. The generic formulas for the two processes are given in reactions (1) and (2), respectively. They are coined as ''alkyl group transfer reactions'', which deal mainly with the alkyl group transfer among different aromatic rings. Such processes are commonly used in the conversion of toluene into benzene and xylenes. Moreover, disproportionation of EB and isopropylbenzene (IPB) yields diethylbenzene (DEB) and dipropylbenzene (DPB), respectively.

Owing to the recent development in catalytic chemistry of zeolites, a drastic improvement in aromatic conversion process technology has been found. There has been a growing research interest in both academic and industry. The results obtained from the fundamental research in turn promote more innovation and development and hence stimulate fine-tuning of zeolite catalyst from the approach of molecular engineering level. For example, several successful processes have been developed for the production of *para*-dialkylbenzenes using zeolitic catalysts. The subject has been reviewed by Weisz [19] and Csicsery [20] on the fundamentals of shape selectivity of catalysis, Kaeding et al. [21] on the Mobil's aromatics processes, Haag et al. [22] on acid catalytic aspects of medium-pore zeolites, and recently, Chen et al. [23] on industrial shape selective catalysis, Venuto et al. [24] on microporous catalysis chemistry, Ribeiro et al. [25] on techniques of zeolite modification, Khouw and Davis [26] particularly on metal encapsulation and in the application of electro- and photo-chemical reactions.

Improving and finding cost effective disproportionation and transalkylation catalytic processes are interesting and challenging tasks in industrial research. In recent years, there have been many research attempts in the area of process development. These new processes not only have had a great impact on process economics, such as production cost and supply and demand of aromatics, but also on the optimum process integration between conversion and separation units in a traditional dialkylbenzene production complex.

Several newly developed novel processes produced dialkylbenzenes which are particularly rich in *para*-isomers compared to their thermodynamic equilibrium compositions, for example, MSTDP^{SM}, MTPX^{SM} and PX-Plus^{SM} for *p*-xylene production [27–30] and TSMC's (Taiwan Styrene Monomer) selective PDEB process for *p*-DEB production [31]. In addition, several new emerging heavy aromatics conversion processes with maximum approach to thermodynamic equilibrium xylene yield have also been developed, namely Tatoray^{SM} [32–34] and TransPlus^{SM} [35–38].

The present review is presented from the perspective of process technology of aromatic interconversion along with fundamental research on shape selective catalysis. In particular, the selection of a suitable zeolite for a process and the fundamentals of shape selective catalysis are intensively discussed. For application point of view, the interplay of market demand and process technology development is reviewed and the development of alkyl group transfer processes from the perspectives of overall economics of production complex is thoroughly discussed. An extensive patent search and industrial process review have been done along with the evaluation of their possible impacts on the production scheme. Moreover, the existing relevant separation technologies are discussed and a perspective on trend in related research and development is included.

2. Zeolite structure

Zeolites are crystalline and porous materials with an open structure that consist of AlO_4 and SiO_4 tetrahedral units linked through oxygen atoms. Owing to their unique pr{o}perties in ion exchange and adsorption capacity and catalytic activity, zeolites have been widely used as adsorbents, molecular sieving agents and catalysts for a variety of different chemical reactions. They have also been modified by isomorphous substitution of silicon and aluminium by incorporating other atoms such as titanium, iron, gallium, boron, phosphorous, etc. in the framework.

There are over 40 known natural zeolites and more than 150 synthetic zeolites have been reported [39,40]. The number of synthetic zeolites with new structure morphologies grows rapidly with time. Based on the size of their pore opening, zeolites can be roughly divided into five major categories, namely 8-, 10- and 12-membered oxygen ring systems, dual pore systems and mesoporous systems [23]. Their pore structures can be characterized by crystallography, adsorption measurements and/or through diagnostic reactions. One such diagnostic characterization test is the ''constraint index'' test. The concept of constraint index, originally introduced by Frilette et al. [41], was defined as the ratio of the cracking rate constant of *n*-hexane to 3-methylpentane. The constraint index of a typical medium-pore zeolite usually ranges from 3 to 12 and those of the large-pore zeolites are in the range

Table 1
Structural characteristics of selected zeolites [23,39]

Zeolite	Number of rings	Pore opening (Å)	Pore/channel structure	Void volume (cc/g)	D_{Frame}[a] (g/cc)	CI[b]
8-membered oxygen ring zeolites						
Erionite	8	3.6×5.1	Intersecting	0.35	1.51	38
10-membered oxygen ring zeolites						
ZSM-5	10	5.1×5.6	Intersecting	0.29	1.79	8.3
		5.1×5.5				
ZSM-11	10	5.3×5.4	Intersecting	0.29	1.79	8.7
ZSM-23	10	4.5×5.2	One-dimensional	–	–	9.1
Dual pore system						
Ferrierite (ZSM-35, FU-9)	10, 8	4.2×5.4	One-dimensional	0.28	1.76	4.5
		3.5×4.8	10:8 intersecting			
MCM-22	12	7.1	Capped by six rings	–	–	1–3
	10	Elliptical	Two-dimensional			
Mordenite	12	6.5×7.0	One-dimensional	0.28	1.70	0.5
	8	2.6×5.7	12:8 intersecting			
Omega (ZSM-4)	12	7.4	One-dimensional	0.38	1.65	0.5
	8	3.4×5.6	One-dimensional			
12-membered oxygen ring zeolites						
ZSM-12	12	5.5×5.9	One-dimensional	–	–	2.3
Beta	12	7.6×6.4	Intersecting	–	–	0.6
	12	5.5×5.5				
Faujasite (X, Y)	12	7.4	Intersecting	0.48	1.27	0.4
	12	7.4×6.5	12:12 intersecting			
Mesoporous system						
VPI-5	18	12.1	One-dimensional	–	–	–
MCM41-S	–	16–100	One-dimensional	–	–	–

[a]Framework density.
[b]Constraint index.

1–3. For materials with an open porous structure, such as amorphorous silica alumina, their constraint indices are normally less than 1. On the contrary, small-pore zeolites normally have a large constraint index; for example, the index for erionite is ca. 38.

A comprehensive bibliography of zeolite structures has been published by the International Zeolite Association [39]. The structural characteristics of assorted zeolites are summarized in Table 1.

Zeolites with 10-membered oxygen rings normally possess a high siliceous framework structure. They are of special interest in industrial applications. In fact, they were the first family of zeolites that were synthesized with organic ammonium salts. With pore openings close to the dimensions of many organic molecules, they are particularly useful in shape selective catalysis [23]. The 10-membered oxygen ring zeolites also possess other important characteristic properties including high activity, high tolerance to coking and high hydrothermal stability. Among the family of 10-membered oxygen ring zeolites, the MFI-type (ZSM-5) zeolite (Fig. 5(A)) is probably the most useful one. ZSM-5 zeolite has two types of channel systems of similar size, one with a straight channel of pore opening 5.3×5.6 Å and the other with a tortuous channel of pore opening 5.1×5.5 Å. Those intersecting channels are perpendicular to each other, generating a three-dimensional framework. ZSM-5 zeolites with a wide range of SiO_2/Al_2O_3 ratio can easily be synthesized. High siliceous ZSM-5 zeolites are more hydrophobic [42] and hydrothermally stable [43] compared to many other zeolites. Although the first synthetic ZSM-5 zeolite was discovered more than two decades ago new interesting applications are still emerging to this day. For example, its recent applications in NO_x reduction, especially in the exhaust of lean-burn engine [44], have drawn much attention. Among various zeolite catalysts, ZSM-5 zeolite has the greatest number of industrial applications, covering from petrochemical production and refinery processing to environmental treatment.

Although the 10-membered oxygen ring zeolites were found to possess remarkable shape selectivity, catalysis of large molecules may require a zeolite

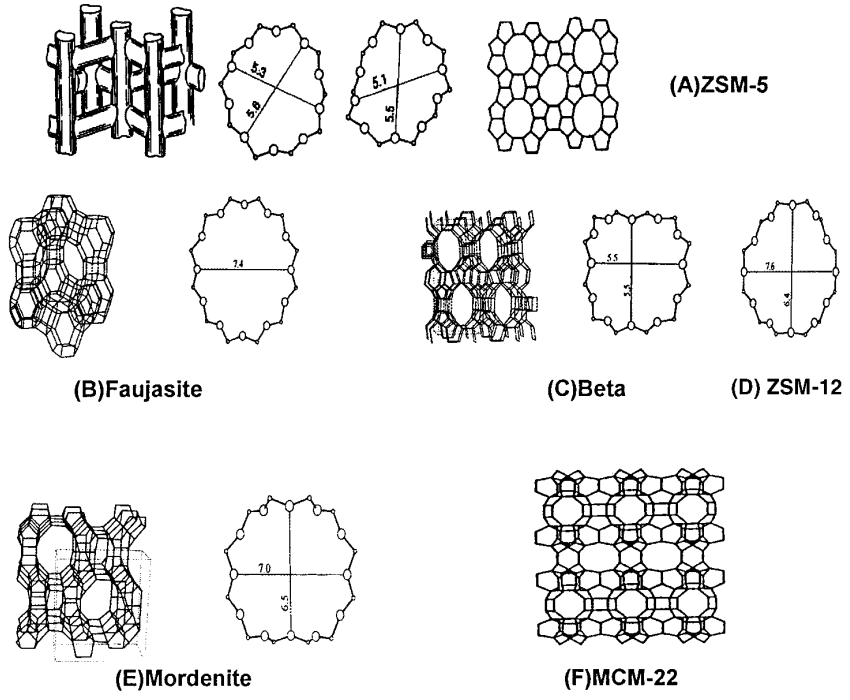

Fig. 5. Framework structure of zeolites: (A) ZSM-5 (B) Faujasite (C) Beta (D) ZSM-12 (E) Mordenite (F) MCM-22; reproduced from refs. [39,45].

catalyst with a larger-pore opening. Typical 12-membered oxygen ring zeolites, such as faujasite-type zeolites, normally have pore opening greater than ca. 5.5 Å and hence are more useful in catalytic applications with large molecules, for example in trimethylbenzene (TMB) conversions. Faujasite (X or Y; Fig. 5(B)) zeolites can be synthesized using inorganic salts and have been widely used in catalytic cracking since the 1960s. The framework structures of zeolite Beta and ZSM-12 are shown in Fig. 5(C) and Fig. 5(D), respectively.

Zeolites with a dual pore system normally possess interconnecting pore channels with two different pore opening sizes. Mordenite is a well-known dual pore zeolite having a 12-membered oxygen ring channel with pore opening 6.5×7.0 Å which is interconnected to 8-membered oxygen ring channel with opening 2.6×5.7 Å (Fig. 5(E)). MCM-22, which was found more recently, also possesses a dual pore system. Unlike mordenite, MCM-22 consists of 10- and 12-membered oxygen rings (Fig. 5(F)) [45] and thus shows prominent potential in future applications.

In the past decade, many research efforts in synthetic chemistry have been invested in the discovery of large-pore zeolite with pore diameter greater than 12-membered oxygen rings. The recent discovery of mesoporous materials with controllable pore opening (from ca. 12 to more than 100 Å) such as VPI-5 [46], MCM-41S [47,48] undoubtedly will shed new light on future catalysis applications.

3. Xylene production process

3.1. Xylene market

Among the three xylene isomers, namely *o*- (1,2-dimethylbenzene), *m*- (1,3-dimethylbenzene) and *p*-xylene (1,4-dimethylbenzene), the last has the great industrial demand. Since *p*-xylene can be used to produce pure terephthalate and polyester, the annual growth production rate of *p*-xylene usually coincides with the gross national production rate (GNP) [3]. There is strong demand especially in countries of the Pacific Rim region. Worldwide growth rates were 7% and 8.8% in the 1990–1995 and 1995–2000 periods, respectively [17]. The application for polyester is comprised of 73% fiber, 14% PET (polyethylene-terephthalate) resin, 7% PET film and 6% miscellaneous [3]. Among them, growth rate of PET resin demand was particularly high, up to around 17% [17]. It is owing to the high growth rate for *p*-xylene in the past decade that many major petrochemical companies worldwide have pursued active *p*-xylene expansion projects to meet the strong market demand [49]. It is expected that the worldwide *p*-xylene production will increase by 50% in the next decade [3,17,18].

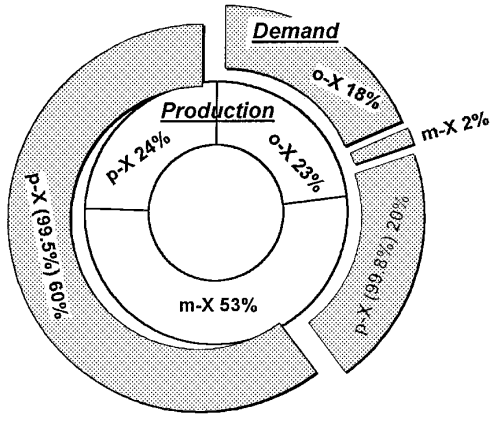

Fig. 6. Spectrum of worldwide production rate and market requirement of xylenes.

By comparison, *o*-xylene produces phthalic anhydride which is used for plasticizer. The average growth rate of *o*-xylene was around 5–9% per year, which was slightly lower than that of *p*-xylene [16,50]. On the other hand, *m*-xylene is mostly used in producing isophthalic acid, which is a valuable additive for polyester. Although the demand for *m*-xylene is low (Fig. 6), it shares the same growth rate as *p*-xylene. While most of the aromatics production processes yield xylene mixtures with a ratio approaching thermodynamic equilibrium, (24:53:23 for *p*-, *m*-, and *o*-isomer, respectively), the market demand for the same xylene isomers is roughly in the ratio of 80:2:18 [13–16], as shown in Fig. 6. Since the amount of *p*-xylene obtained directly from the reaction mixtures cannot meet market requirement, the surplus *m*-xylene and *o*-xylene are further isomerized to *p*-xylene to balance the market demand.

3.2. Recovery of p-xylene and o-xylene

By convention, the so-called C_8 aromatics (A_8) include four isomers, namely *o*-, *m*- and *p*-xylene

Table 2
Physical properties of dialkylbenzne aromatics [15,51]

Isomer	Boiling point (°C)	Melting point (°C)	d_4^{20}
Dimethylbenzenes (C_8 aromatics)			
Ethylbenzene	136.2	−95.0	0.8670
p-Xylene	138.3	+13.3	0.8611
m-Xylene	139.1	−47.9	0.8642
o-Xylene	144.4	−25.2	0.8802
Methylethylbenzenes (C_9 aromatics)			
p-Ethylmethylbenzene	162.0	−62.4	0.8656
m-Ethylmethylbenzene	161.3	−95.6	0.8689
o-Ethylmethylbenzene	165.2	−80.8	0.8851
Diethylbenzenes (C_{10} aromatics)			
p-Diethylbenzene	183.8	−42.9	0.8670
m-Diethylbenzene	181.1	−84.2	0.8684
o-Diethylbenzene	183.5	−31.2	0.8839
Methylpropylbenzene isomers (C_{10} aromatics)			
p-Methylisopropylbenzene	177.1	−67.9	0.8615
m-Methylisopropylbenzene	175.1	−63.7	0.8652
o-Methylisopropylbenzene	178.2	−71.5	0.8808
p-Methyl-*n*-propylbenzene	183.3	−64.2	0.8631
m-Methyl-*n*-propylbenzene	181.8	−82.2	0.8659
o-Methyl-*n*-propylbenzene	184.8	−60.2	0.8783
Dipropylbenzenes (C_{12} aromatics)			
p-Diisopropylbenzene	210.5	−17.1	0.8606
m-Diisopropylbenzene	203.2	−63.1	0.8629

and ethylbenzene (EB). As shown in Table 2 [51], these four isomers all have similar physical properties. In comparing its vast demand to the other A_8 isomers (Fig. 6), *p*-xylene recovery plays the key role in determining the A_8 separation scheme.

EB has the lowest boiling point but it is only 2.1°C lower than that of *p*-xylene. Conventionally, it can be recovered by a superfractionation method developed in the 1960s. For example, for a fractionation tower design to have a recovery rate of 95%, it required about 330 theoretical trays and a reflux ratio up to 90. As a result, the requirements for large number of trays and high reflux ratio inevitably resulted in a substantial increase in the recovery cost which is the main reason for the near obsoleteness of the superfractionation method.

The latest technology for EB separation is UOP's Sorbex™ [52] which involves recovery from an A_8 mixture. However, benzene ethylation has become the major source of EB due to its lower production cost and the growing demand of the styrene industry. Thus, a state-of-the-art aromatics complex no longer separates EB from A_8 mixtures. Instead, EB is converted to other A_8 isomers by isomerization reaction or to benzene by dealkylation reaction.

A typical aromatic production scheme (Fig. 7) normally consists of:

1. aromatics production section which includes reforming process and pyrolysis gasoline,
2. extraction section to separate BTX aromatics from non-aromatics raffinate,
3. toluene conversion section which includes disproportionation and transalkylation processes,
4. product recovery section which consists of separation towers of benzene, toluene, xylenes, *o*-xylene and A_9 (C_9 aromatics),
5. *p*-xylene recovery section by either crystallization or adsorption method [4,53–58] and
6. isomerization section for converting raffinate of the *p*-xylene recovery section into xylene isomers.

Typical commercial specifications of some of the aromatics products are presented in Table 3.

3.2.1. *o*-Xylene recovery

o-Xylene has the highest boiling point and is 5.3°C higher than that of *m*-xylene (Table 2). *o*-xylene plus C_9^+ aromatics can first be separated out from the other three isomers in the xylene column. A typical xylene column design normally has 80–160 trays with a reflux ratio of 2–6. Moreover, the system usually maintains a low (30–50%) *o*-xylene recovery rate to prevent contamination of *o*-xylene product and to minimize energy consumption of the xylene splitter [59]. High purity *o*-xylene can then be obtained with a purity up to 98.5% by separating out A_9^+ in the bottom of *o*-xylene column.

Table 3
Product specifications of assorted commodity aromatics

Product	Specification minimum purity (%)
Benzene	99.85
Toluene	99.0
o-Xylene	98.5
p-Xylene	99.5% (typical), 99.8% (ultra-pure)
m-Xylene	99.5
Cumene	99.9
p-Diethylbenzene	97–99

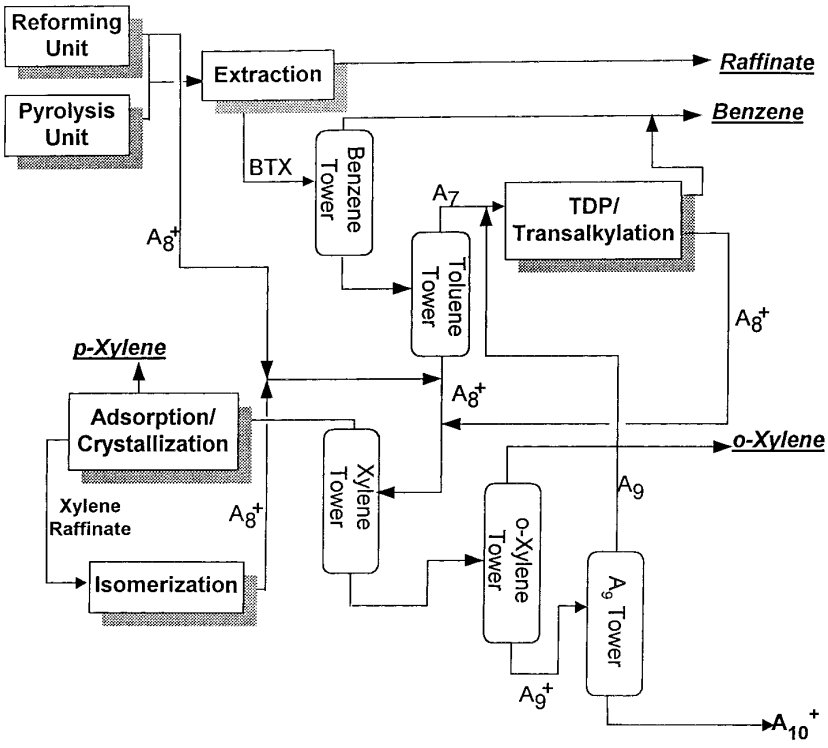

Fig. 7. Typical aromatics production scheme.

3.2.2. p-Xylene recovery

The mixture of EB, *p*-, *m*-xylene, and some residual *o*-xylene, which is collected from xylene splitter top (Fig. 7), is subject for recovering *p*-xylene. The recovery of *p*-xylene from an A_8 mixture can be achieved either by crystallization or adsorption technology.

The more conventional crystallization method takes the advantage of the fact that *p*-xylene has the highest melting point among the A_8 isomers (Table 2). Several practical technologies are known, for example, Isofining^{SM} (Esso), Antar^{SM} (HRI, Hydrocarbon Research) and the proprietary processes developed by Krupp Koppers, Maruzen and ARCO (Atlantic Richfield). Conventionally, the crystallization process operates at low temperature and utilizes a two-stage crystallizer scheme [60]. In the first stage the crystallizer, which is maintained in the temperature range from $-60^{\circ}C$ to $-70^{\circ}C$, yields only a wet cake with a relatively low *p*-xylene purity. During this stage, *m*- and *p*-xylene together form an eutectic mixture which limits the lowest crystallization temperature [61]. Refrigeration cost increases substantially with the temperature below $-35^{\circ}C$, at which ductility of the insulation material becomes an issue [62]. The temperature of the eutectic mixture controls *m*-xylene impurity levels and the maximum recovery rate of *p*-xylene. As shown in Fig. 8 [63], eutectic temperatures can be calculated from the ratio of the concentration of *m*-xylene to the concentration of *p*-xylene in the feed and the ratio of the concentration of *m*-xylene and of *p*-xylene in eutectic mixtures. The eutectic temperature of thermodynamic equilibrium xylene compositions with *p*-xylene to *m*-xylene concentration ratio of 0.45 is $-52.6^{\circ}C$ [63,64]. It increases with higher concentrations of *p*-xylene, EB and *o*-xylene in A_8 mixture [63]. In the second stage the crystallizer is operated in the temperature range from $-18^{\circ}C$ to $4^{\circ}C$. This further purifies the wet cake generated in the first stage. The wet cake from the second stage is then further washed with *p*-xylene or toluene to obtain *p*-xylene with 99.5% purity. The two-stage crystallizer scheme described above is operated at a high recycle rate of mother liquid. As shown in Fig. 9, for typical thermodynamic equilibrium xylene compositions, the

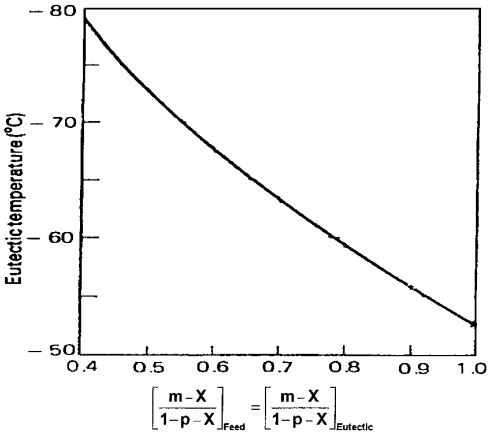

Fig. 8. Relationship between eutectic temperature and ratio of *m*-xylene and *p*-xylene compositions in feedstock and eutectic mixtures; reproduced from ref. [63].

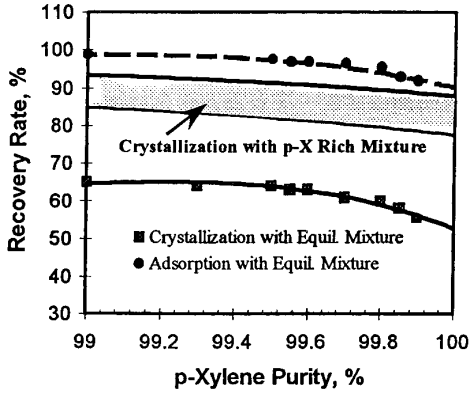

Fig. 9. Schematic comparison of *p*-xylene recovery rate of different compositions of xylene mixtures by crystallization and adsorption methods; data from refs.[30,53,78].

p-xylene recovery rate obtained by crystallization is ca. 65%, as compared to the value of 90–95% obtained by adsorption. The low recovery rate and low crystallization temperature of the former resulted in an operating cost 2–6 times higher than the latter technique [53]. Worldwide unit capacity applying crystallization technology is excessively lower than that applying adsorption technology, accounting for 35% and 65% global *p*-xylene capacity, respectively [30].

The adsorption method mostly utilizes modified faujasite as the adsorbent over which *p*-xylene has the greatest adsorption affinity among the species in the isomer mixture [53,54]. Several industrial technologies are known, for example, Parex^{SM} (UOP), Aromax^{SM} (Toray) and Eluxyl^{SM} (IFP). The adsorption process is operated in a simulated moving, countercurrent, liquid phase adsorption bed at constant chamber temperature and pressure [4,63,65], with typical ranges of 160–180°C and 8–12 atm [63]. Separation proceeds through four zone steps, namely adsorption zone, purification zone, desorption zone and buffer zone along the axial positions of adsorption chamber [53,65] in which *p*-xylene concentration changes with sequential time and chamber positions. The control of the sequential operations is the key characteristics of different technologies. Parex^{SM} Process applies a patented rotary valve, which is a multiport valve. A rotary valve comprises connectors of various bed line pipes to deliver liquids of changing concentrations into various zones of the adsorption chamber and product distillation towers and feed lines. The adsorption process requires a stringent specification of A_9^+ content.

Design of Eluxyl^{SM} Process has two versions, a stand-alone version and a so-called hybrid version [54–58]. In the stand-alone version, *p*-xylene was recovered directly from xylene mixtures by the adsorption unit. The hybrid version consists of an adsorption unit and a crystallizer in which *p*-xylene purity is upgraded first by the adsorption unit from thermodynamic equilibrium composition (with 23% concentration) up to ca. 90%, and that product is then purified by crystallization to 99.5%+ purity. The stand-alone version applies five zones as the adsorption configuration [54], which has one additional adsorption stage more than Parex^{SM} Process. In contrast, the hybrid version applies four zone configurations. It was claimed that the hybrid version has higher productivity, with smaller adsorbent inventory and requires fewer fractionation columns.

After the recovery of *p*-xylene, the remaining isomer mixture, namely A_8 aromatic raffinate, is subject to isomerization which converts the *p*-xylene lean raffinate into a thermodynamic equilibrium mixture (Fig. 7). The mixture is then recycled back to the separation scheme loop for extinct recovery of *o*-xylene and *p*-xylene. The typical flow rate of the recycling loop is about three times larger than the fresh A_8 mixture.

The key factors which affect the *p*-xylene recovery rate and purity vary with the recovery technique used.

In the case where the crystallization method is applied, the *p*-xylene recovery rate is found to depend on the overall xylene composition, which dictates the temperature limit of the eutectic mixture. In the case of the adsorption method, however, the recovery rate has a strong dependence on the EB content which has a similar adsorption affinity to *p*-xylene over the zeolite adsorbent [53,54].

There has been a growing demand from the downstream PTA (pure terephthalic acid) industries to upgrade the *p*-xylene purity specification. For example, high purity *p*-xylene is indispensable for the production of PET bottle resins and microfiber polyester. As a result, the purity specification of *p*-xylene has increased from 99.2% in the 1970s to 99.8% in the 1990s [66]. Nowadays, ultra-high purity *p*-xylene occupies about 20% of the worldwide xylene market, as shown in Fig. 6. It is believed that the *p*-xylene recovered by the state-of-art adsorption technology alone is capable of meeting the growing market demand and purity requirements [66]. Since the energy consumption cost for *p*-xylene recovery by the crystallization method is much higher and much more sensitive to product purity than that of the adsorption technique (Fig. 9), the conventional crystallization method has been gradually replaced by the adsorptive separation process. However, recent advances in *p*-xylene selective disproportionation processes seem to favor more on the crystallization method; their impacts are discussed below.

3.3. Toluene disproportionation

3.3.1. Commercial disproportionation processes

There are two major techniques to convert surplus toluene into other aromatics. The first is methyl group transfer, are shown earlier in reactions (1) and (2) with the R group representing methyl group. The second (reaction (3))is hydrodealkylation.

Hydrodealkylation

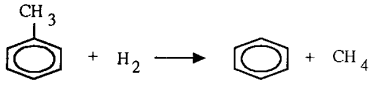

(3)

The methyl group transfer technologies, which include disproportionation and transalkylation, convert toluene into benzene and xylenes simultaneously whereas the hydrodealkylation scheme mainly produces benzene. From the data in Fig. 10, it is obvious that there is a growing demand for methyl group transfer technologies than for the hydrodealkylation process mainly due to the growing xylene market and partially from the impact of freeing up of benzene from RFG regulation [12]. In the US market, the annual growth rates of disproportionation process and hydrodealkylation were 6.9% and 0.7%, respectively [18]. Compared to the methyl group transfer reactions, hydrodealkylation processes are normally operated at a much higher reaction temperature (ca. 650°C) and require higher operation and capital investment cost by about 10% [16].

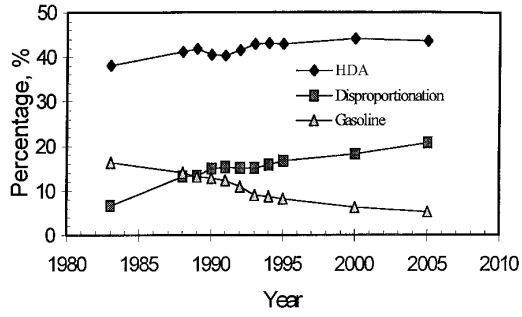

Fig. 10. Worldwide growth curves of distribution of toulene usuage for hydrodealkylation and disproportionation processes and gasoline.

Disproportionation and transalkylation are both acid catalyzed reactions. In the early days, liquid Friedel–Crafts [67] and HF–BF_3 systems [68] were commonly used. Then, the metal oxide catalysts, such as CoO–MoO_3 on aluminosilicate/alumina [69] and noble metal or rare earth on alumina were developed and used [70]. In modern technology, zeolite catalyst systems, for example zeolite Y, mordenite, ZSM-5 and other large-pore zeolites, are predominant [71]. Transalkylation processes are normally catalyzed by large-pore zeolites which can also be used for toluene disproportionation. The latter, however, is mostly catalyzed by 10-membered oxygen ring zeolites having medium-pore size such as ZSM-5 zeolite.

The main products of toluene disproportionation are benzene and xylenes. In addition to main reaction, there are some side reactions, including xylene disproportionation producing A_9 and dealkylation of alkylbenzenes producing light gas. Therefore, characteristics of the catalytic processes include conver-

Table 4
Summary of commercial toluene disproportionation processes

	Process name				
	TDP-3 [73]	MSTDP [27]	MTPX [79]	PX-Plus [30]	T2BX [74]
Developer	Mobil	Mobil	Mobil	UOP	FINA
Catalyst	ZSM-5	ZSM-5 pre-coked	ZSM-5 silica modified	Not disclosed	Not disclosed
Reaction conditions					
Reactor type	Fixed bed	Fixed bed	Fixed bed	Fixed bed	Fixed bed
Temperature (°C)	435	455–470	~420	–	390–495
Pressure (kg/cm^2)	24.5–28.2	21.1–42.3	~21.1–42.3	–	49.3
H_2/HC (mol)	1–2	2–4	~2–4	–	4
WHSV (h^{-1})	6	2–4	–	–	1.2–2.3[a]
Conversion (%)	45–50	30	30	30	44
Product Selectivity (%)[b]					
C_5^- gas	2.7	6.6	3.7	5.3	8.1
Benzene	42.3	44.9	44.7	46.4	35.0
Xylenes	50.4	43.5	48.0	44.7	40.8
EB	1.3	2.5	2.0	1.9	2.4
C_9^+ aromatics	3.3	2.5	1.6	1.7	13.7
Xylene distribution (%)[c]					
p-Xylene	25.2	82.2	89.8	90.2	25.1
m-Xylene	52.8	15.1	8.2	8.5	50.1
o-Xylene	22.0	2.7	2.0	1.4	24.8
B/(X+EB) (mol)	1.1	1.3	1.2	1.4	1.1
Cycle length (years)	>3	>1.5	–	–	>1

[a] WHSV was estimated from reported LHSV data of 1–2.
[b] Selectivity of PX-Plus was an approximation.
[c] Xylene distribution of MSTDP was line out data in start-of-run period.

sion, product yields and reaction conditions and, more importantly, throughput.

The typical operating conditions for most commercial disproportionation processes are depicted in Table 4. Among the well-known Mobil disproportionation processes, the Toluene Disproportionation Process version 3 (TDP-3^{SM}) is known for its high catalyst activity, high stability and low EB yield [72,73], which would reduce the recovery cost of *p*-xylene in downstream units. Compared to the earlier ZSM-5 technology, the TDP-3^{SM} Process can lower reaction temperature about 50°C [73]. Its space velocity is the highest one among the known processes (Table 4). Selectivity is good, having benzene-to-xylene molar ratio of 1.1, which is close to the theoretical number of unity. Its first cycle length is more than three years. The reactor can be radial or axial flow design. The TDP-3^{SM} can process toluene feed containing feed up to 25% A_9.

The T2BX^{SM} Process, which Fina Oil developed in the 1980s [74], applied severe operating conditions, such as lower space velocity. Water content is limited to 250 ppm and hydrogen consumption was around 17.8 m^3/m^3 feed. It produced excessively high amounts of A_9 aromatics with selectivity up to 14% (Table 4), which is used as a gasoline blending stock. Recently, Fina Oil made improvements on the process [75].

There are three *p*-xylene selective processes, including the Mobil's Selective Toluene Disproportionation Process (MSTDP^{SM}), (which utilizes ZSM-5 zeolite that is modified by pre-coking treatments [27,76,77]) and Mobil's Toluene to *para*-Xylene (MTPX^{SM}) Process and PX-Plus^{SM} Process, which are known in less detail. According to the patent literature, the ZSM-5 zeolite used in the MTPX^{SM} Process involves a silica selectivation treatment [78,79]. The PX-Plus^{SM} Process incorporated a pro-

prietary selectivation technique, which has not been disclosed to the public. As a result of selectivation, they all produce xylene mixtures with *p*-xylene concentration far beyond its thermodynamic equilibrium value. The relevant details of these processes will be discussed in the next section.

3.3.2. Development of selective toluene disproportionation process

The development of a dialkylbenzene process with enrichment of the *p*-isomer is a challenging technological task. Nonetheless, the pioneering works to improve *para* selectivity started in the 1970s. Yashima et al. [80] observed *p*-xylene selectivity of 45–50%, higher than its thermodynamic equilibrium value, over cation-exchanged zeolite Y. Chen et al. [81,82] found that with a shape selectivity catalyst, *p*-xylene selectivity tended to increase with increasing ZSM-5 crystal size. Since then, more techniques involving modified zeolite catalysts were applied to increase *p*-isomer selectivity.

A number of different modification techniques were found to be useful. Kaeding et al. [83–86] found that impregnating phosphorous, silica, calcium or MgO or boron onto ZSM-5 could enhance the selectivity of *p*-xylene. Large amine molecules, such as 4-methylquinoline [87], 1-methylisoquinoline [88], etc., can be adsorbed only on the zeolite external surface, and improve *para*-isomer selectivity. Since the amines desorb at higher temperatures, the method is applicable only at low reaction temperatures. Germanium was the other modification agent for fine-tune zeolite pore structures; it introduced metal catalytic function into zeolite acid function [89,90]. In terms of external surface coverage, germanium gave less complete coverage than silica [90]. Industrial application applied mainly pre-coking and silica deposition techniques, with proper selection of crystal size, Si/Al ratio and morphology of the parent zeolite.

The basic principles of *para* selectivity improvement include the reduction of diffusivity and the inactivation of external surface sites. While the *p*-isomer is the apparent primary product leaving the zeolite pore mouth [91], isomerization proceeds as the secondary reaction on the zeolite external surface. Since sites located on the external surface are more accessible than the sites in zeolite pores [92], inactivation of external sites can inhibit secondary isomerization and retain the *p*-xylene selectivity in products coming out from zeolite pores.

Diffusivity in zeolites varies widely with molecular structure configurations. For example, it drops sharply in ZSM-5 as the number of branch chains increases (Fig. 11), such as from *n*-hexane to 3-methylpentane over the range of 10^{-4}–10^{-5} cm^2/s, and also as the sizes of alkylbenzenes becomes larger, such as *p*-xylene to *o*-xylene over the range of 10^{-7}–10^{-10} cm^2/s [22,93]. The diffusion rate of *p*-xylene is at least 1000 times faster than that of the other isomers; the increasing diffusion resistance will create more diffusion superiority for *p*-xylene and conversely, more diffusion barrier for *o*-xylene and *m*-xylene. Therefore, *p*-xylene rapidly diffuses out from zeolite pores, inside of which isomerization takes place steadily toward equilibrium to provide additional *p*-xylene isomer for diffusion out. The criteria in coupling of isomerization rate and diffusion rate to enhance *p*-xylene selectivity is [91]

$$D_p \gg D_{m,o} \tag{4.1}$$

$$K_{\mathrm{I}} \geq D_{m,o}/r^2, \tag{4.2}$$

$$K_{\mathrm{D}} \leq D_{\mathrm{T}}/r^2, \tag{4.3}$$

$$(K_{\mathrm{I}}/K_{\mathrm{D}})_{\mathrm{observed}} \leq 1, \tag{4.4}$$

where K_{I} and K_{D} are the rate constants of isomerization and disproportionation, respectively, $D_{m,o}$ and D_{T} are the diffusivities of *m*-xylene or *o*-xylene and toluene, respectively, and r is the crystal size. The ratio of the intrinsic kinetic rate of isomerization reaction to the disproportionation reaction, $K_{\mathrm{I}}/K_{\mathrm{D(intrinsic)}}$, is about 5000 [71]. The ratio of the observed kinetic rates, $K_{\mathrm{I}}/K_{\mathrm{D(intrinsic)}}$, depends on the zeolite pore opening and thus, the constraint index. Moreover, for ZSM-5 zeolite, $K_{\mathrm{I}}/K_{\mathrm{D}}$ decreased from 360 in small crystals to 2 in large crystals, in which the criteria of reaction (4.4) were fulfilled and *para* selectivity was obtained [22,86].

Olson et al. [91] studied the relationship between *p*-xylene selectivity and the diffusion time of *o*-xylene over various ZSM-5 catalysts, including large crystals and small crystals modified with silica, coke, antimony, magnesium, calcium, zinc and boron, as shown in Fig. 12. Diffusivity was expressed with a characteristic diffusion time, $t_{0.3}$, required to sorb 30% *o*-xylene at 120°C, and *para* selectivity was achieved

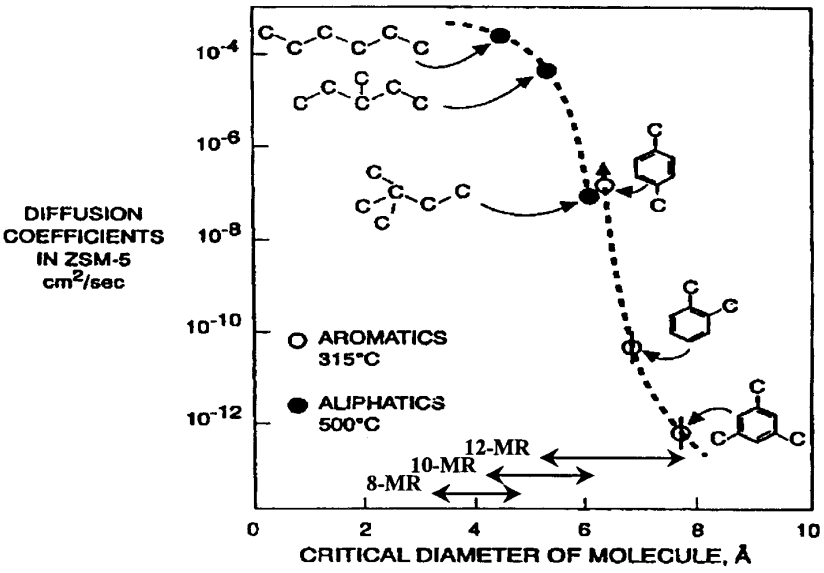

Fig. 11. Diffusion rate of various aliphatics and aromatics molecules over ZSM-5, with comparison to the pore openings of 8-MR, 10-MR and 12-MR zeolites; from ref. [93].

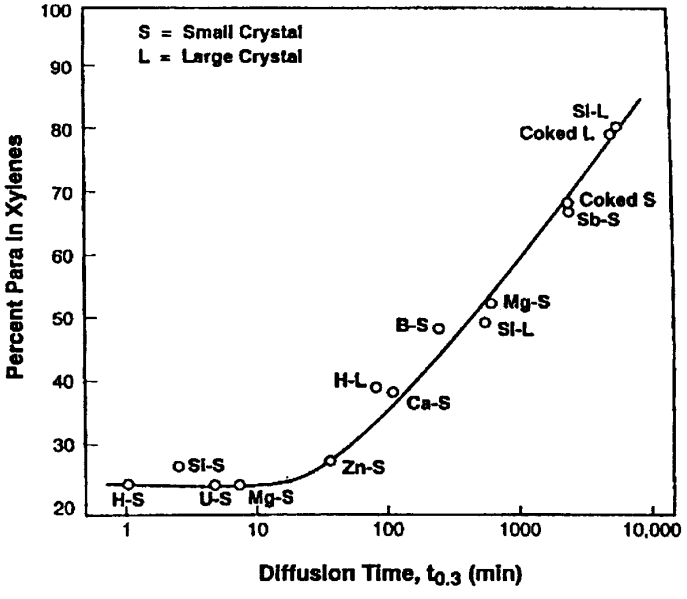

Fig. 12. Relationship between *p*-xylene selectivity in toluene disproportionation over ZSM-5 and their characteristic diffusion time $t_{0.3}$ (adsorption time to adsorb 30% *o*-xylene at 120°C); reaction conditions: 550°C, 41 bar, 20% conversion; reproduced from ref. [91].

only at $t_{0.3}$ beyond around 50 min. Therefore, the diffusivity control mechanism is a useful working principle in assessing *p*-isomer selectivity. Among those modification methods, large crystal size generally produced better *para* selectivity than small crystals. Furthermore, pre-coking pretreatment can effectively enhanced *para*-isomer selectivity up to 70–80% (Fig. 12). It was believed that coke selec-

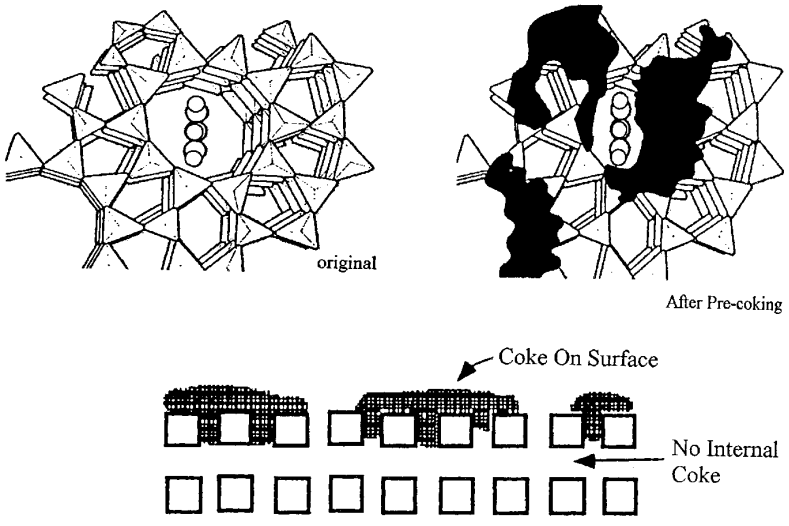

Fig. 13. Coke selectivation conceptual model; reproduced from ref. [91].

tively lays down on the external surface, and inactivates the external active sites, as shown in Fig. 13. Because there is no internal coke deposition, precoking treatment can retain adequate acid sites to catalyze reactions. Mathematical models supported well the conclusion, showing that *p*-xylene concentration is greater than 90% when conversion is low and effectiveness factor, $(Kr^2/D)^{1/2}$, is greater than 10 [94,95]. A schematic model (Fig. 14) illustrated the working principle, showing the relative diffusivity of xylene isomers and rate constants of isomerization and disproportionation.

However, there were disagreements about the key controlling parameters among these above-mentioned parameters. Bhat et al. [96,97] proposed that inactivation of external surface is the prominent control strategy for achieving high *para*-isomer selectivity. Wang et al. [87] concluded in the studies of EB disproportionation and toluene ethylation that *para*-isomer selectivity was not solely dependent on diffusion barrier and that external surface inactivation was another important factor. They also found that the modification requirement for *para*-isomer selectivity enhancement varies with reaction types. Niwa et al. [98–101] have conducted extensive studies on the working mechanisms of *para*-isomer selectivity enhancement of toluene methylation. They prepared various parent zeolite samples with different Si/Al

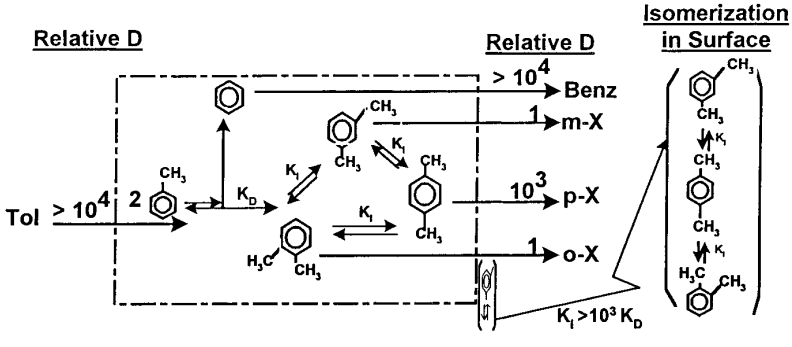

Fig. 14. Conceptual model of selective toluene disproportionation over ZSM-5 (modified from refs. [19,22,24,71,84,86,91].

ratios and crystal sizes, on which silica CVD modification was performed. Silica covers the external surface and also reduces the effective pore size by ca. 0.1 and 0.2 nm upon the formation of 1, 2 and 3 molecular layers of silicon oxide [101]. All the samples were characterized by diffusion rate measurements, 1,3,5-triisopropylbenzene cracking tests and *o*-xylene isomerization tests. They concluded from the extent of dependency of *para*-isomer selectivity enhancement on characterization properties that narrowing of the pore opening is much more important than the inactivation of external surface. On the other hand, Yashima et al. [102] reported that weaker acidity in metal MFI zeolites catalyzes higher *para* selectivity and the working parameter is different for disproportionation of alkylbenzenes and aromatics alkylation [103]. Nevertheless, *para* selectivation depends on various factors, such as morphology of the starting zeolite sample, type of reaction, details of modification techniques, etc.

Haag et al. [76,77] disclosed a coke selectivation technique over ZSM-5 zeolite to enhance *p*-xylene selectivity up to 79% during toluene disproportionation. The requirements of treatment time to achieve 40% and 60% *p*-xylene selectivity are shown in Fig. 15 [76]. Effectiveness of the pre-coking treatment increases with increasing coking temperature but raises concerns of catalyst stability. Pretreatment time would be longer than six days with the pre-coking temperature below ca. 520°C. The H_2/HC ratio during pre-coking treatment is also found to have substantial effect on *p*-xylene selectivity. As shown in Fig. 16, pre-coking time requirements increase dramatically

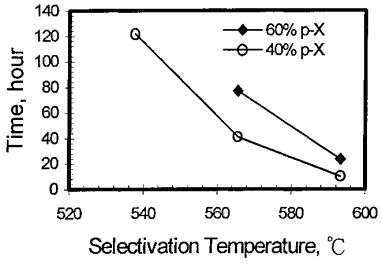

Fig. 15. Effects of selectivation temperature in pre-coking treatment on the requirement of pre-coking time for achieving various *p*-xylene selectivity; reaction conditions: WHSV: 6.5–20 h^{-1}, H_2/HC=0.5 mol/mol, N_2/HC=3.5 mol/mol, Pressure: 28.2 kg/cm^2; Data from ref. [77].

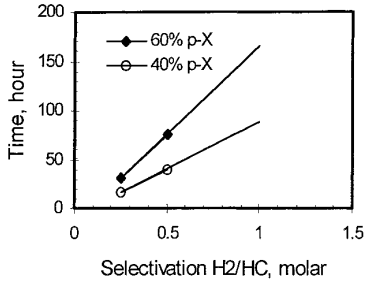

Fig. 16. Effects of selectivation H_2/HC in pre-coking treatment on the requirement of pre-coking time for achieving various *p*-xylene selectivity; reaction conditions: temperature: 566–593°C, WHSV: 13–20 h^{-1}, N_2/HC=3.5 mol/mol, pressure: 28.2 kg/cm^2; data from ref. [77].

with increasing H_2-to-aromatics ratio. Pre-coking was not practical to enhance *para*-isomer selectivity at H_2-to-aromatics molar ratio beyond ca. 0.7. According to the patent literature, the typical pre-coking temperature is about 55–100°C higher than the normal reaction temperature. As a result, the pre-coking treatment incorporated 15–25% of coke onto the zeolite [76] and enhanced the *p*-xylene selectivity to 70–80%.

The pre-coking treatment process was industrially applied in the so-called MSTDP^{SM} Process. Its performances in the first and second cycles were shown in Figs. 17–19 [27]. Its start-up took 37 h for coke selectivation at reactor inlet temperature, possibly higher than 500°C (Fig. 17). Reaction temperature was lined out at 455°C in the start-of-run period, and gave *p*-xylene selectivity of 82% at 30% toluene conversion (Fig. 18). The cycle length was over one and half years. At end-of-run period, *p*-xylene selectivity increased with day-on-stream to 90% with 25% toluene conversion, after which regeneration was

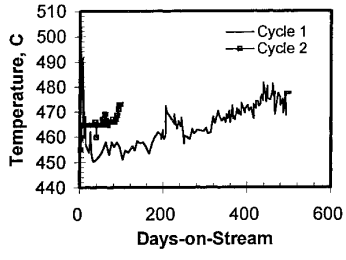

Fig. 17. Plot of reaction temperatures against days-on-stream in MSTDP commercial unit; feed: toluene, WHSV: 2–4 h^{-1}, H_2/HC: 2–4 mol/mol, adapted from ref. [27].

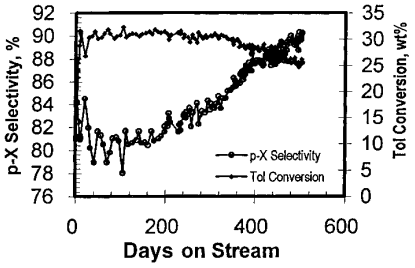

Fig. 18. First cycle performance of MSTDP commercial unit by plotting *p*-xylene selectivity against toluene conversion; WHSV: 2–4 h^{-1}, adapted from ref. [27].

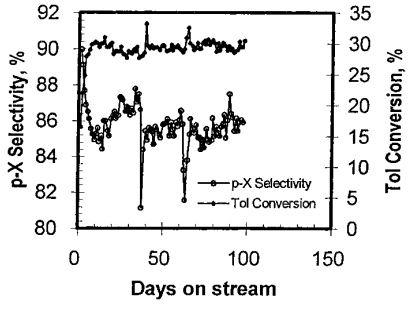

Fig. 19. Second cycle performance of MSTDP commercial unit by plotting *p*-xylene selectivity against toluene conversion; WHSV: 2–4 h^{-1}; adapted from ref. [27].

required. It was noted that the catalyst used in the MSTDP^{SM} could be completely regenerated. The start-of-cycle temperature of the second cycle was about 465°C, with a *p*-xylene selectivity of 86% (Fig. 19). Comparing to TDP-3^{SM} Process, MSTDP operation is lower in throughput, and higher in reaction temperature, resulting in a higher benzene-to-xylene molar ratio of 1.3 and higher light gas yield (Table 5). Nevertheless, in a process economics evaluation, MSTDP^{SM} is more competitive than TDP-3^{SM}, mainly from improvement in *p*-xylene selectivity and *p*-xylene recovery cost [12,30].

Although pre-coking technique was successfully used industrially, there were only a few mechanistic studies [85,86,91,104–106]. Olson et al. [91] proposed that coke tends to deposit on the external surface of ZSM-5 (Fig. 13) and passivates the isomerization on external surface. Chen et al. [104] proposed that for fresh ZSM-5 catalyst during early time on stream coke is formed preferentially on Brønsted acid sites that are located in the channels. Fang et al. [105] further demonstrated that the nature and location of coke in toluene disproportionation can be manipulated by a five-stage on-stream treatment with switching different carrier gases (between nitrogen and hydrogen) under varied temperatures in range of 480–540°C (Fig. 20). During the test periods, conversion drops in nitrogen gas and recovers in hydrogen, while *p*-

Table 5
Selectivation of toluene disproportionation over ZSM-5 [79]

Treatment	Unmodified	DMS modified[a]	PMS modified[a]	Pre-coking
Days-on-stream	91	9	63	–
WHSV (h^{-1})	8	6	7	4
Temperature (°C)	404	439	422	446
Pressure (kg/cm^2)	42.2	42.2	42.2	35.2
H_2/aromatics (mol/mol)	2	2	2	2
Conversion (%)	30.9	28.6	30	30.9
Yield (%)				
C_5^- gas	0.3	0.7	1.1	1.7
Benzene[b]	12.9	12.2	13.4	14.0
Xylenes	17.0	14.8	15.0	14.8
C_9^+ aromatics	0.7	0.9	0.5	0.4
Benzene/xylene (mol)	1.0	1.1	1.2	1.3
p-Xylene selectivity (%)	26.1	56.9	86.0	85.0

[a] 10% modifier silica, H–ZSM-5/silica binder.
[b] By balance of original data.
[c] *p*-Xylene at thermodynamic equilibrium composition is 23.4%.

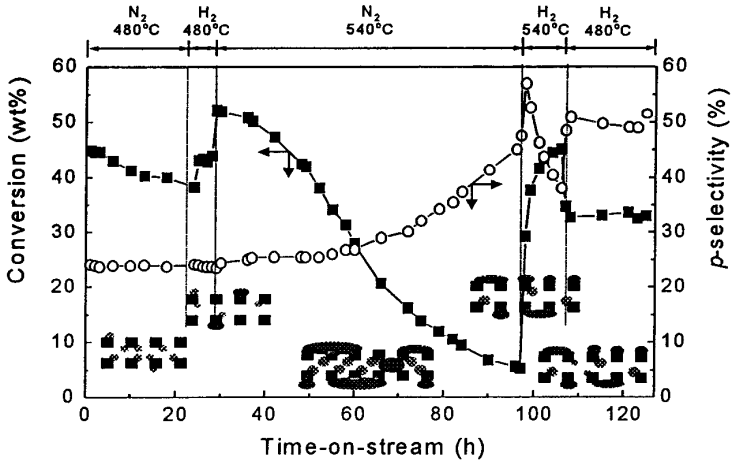

Fig. 20. Conversion and *p*-xylene selectivity in toluene disproportionation over ZSM-5 with five stage coke selectivation treatment; reaction conditions: WHSV: 6.5 h^{-1}, carrier gas/toluene: 4 mol/mol, pressure: 28.2 kg/cm^2; from ref. [105].

xylene selectivity remains fairly constant in initial stages, Stages I and II, and is enhanced along with catalyst deactivation in Stage III as shown in Fig. 20. From measurements on coked catalyst samples from various stages, the coke laydown process involves coke migration and rearrangement. As shown in Fig. 20, in Stage I by using nitrogen, coke deposits preferentially inside zeolite pores, with small inhomogeneous deposition occurring externally. In Stage II, by switching to hydrogen, internal coke was stripped out to external surface, resulting in reduction of total coke content. In Stage III by using nitrogen, coke deposited heavily inside zeolite pores, and on the external surface and pore openings, leading to severe deactivation in catalyst activity, with a gradual improvement in *p*-xylene selectivity. In Stage IV by switching to hydrogen, similarly to Stage II, internal coke was stripped out toward the external surface, resulting in a large coverage of the external surface. Catalyst activity restored and *p*-xylene selectivity stayed high. As evidenced by ^{129}Xe NMR measurements, with coke content of 19%, there was no pore opening change, whereas void space was 94% of the original level. In Stage V, reaction temperature was reduced to extend normal operation cycle, coke laydown rate was slow, and *p*-xylene selectivity remained high. Their work indicated clearly that coverage of external surface sites contributes to *p*-xylene selectivity enhancement in toluene disproportionation at medium *para*-isomer selectivity, ca. 50%.

Surface modification by silica deposition is the other widely applied industrial practice to improve *para* selectivity over ZSM-5. It is believed that the catalyst applied industrially in the MTPX^{SM} Process was silica modified. Such modification can be achieved either by *in situ* silica deposition or *ex situ* impregnation. The effectiveness of silica deposition depends on the silica sources, deposition methods, and also the nature of the zeolite raw material. Impregnation is conducted either using organic solutions (particularly in hexane, decane and dodecane) of organic silicones onto parent ZSM-5 either synthesized with [79,107–111] or without organic templates [112], or with water emulsion of silicones [79,113–115]. Multiple-impregnations [116–118] followed by steaming [119,120] are also applied as pretreatment procedures. Interestingly, steaming *alone* gives no improvement in *para*-isomer selectivity; in contrast, steaming treatment at mild conditions, ca. 2 h at 340°C, following silica impregnation can enhance catalyst activity and also reduce D/r^2 ratio to enhance *p*-xylene selectivity [116,120]. Significant improvement in *p*-xylene selectivity is obtained with various modifications achieving D/r^2 ratio lower than ca. 10^{-7}–10^{-8} s^{-1} in comparison to the original samples at 10^{-5} s^{-1} [111,112,116,120].

Chang et al. [79] used different silica compounds such as phenylmethylsilicone (Dow-710^{TM}, PMS), dimethylphenylmethylpolysiloxane (Dow-550^{TM}), or dimethylsilicone (DMS) as impregnation treatment agents to improve *p*-xylene selectivity. As shown in

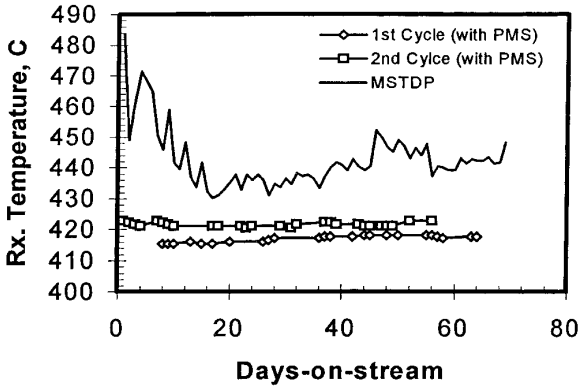

Fig. 21. Plot of reaction temperature against days-on-stream by using silica selectivation (cycles 1 and 2) and pre-coking selectivation to achieve comparable toluene conversion and *p*-xylene selectivity various modification treatments; data from refs. [27,79].

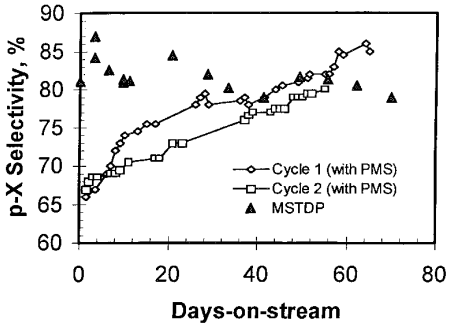

Fig. 22. Plot of *p*-xylene selectivity of silica deposition selectivation method (cycles 1 and 2) against days-on-stream in comparison to pre-coking selectivation method; reaction conditions: temperature: 422°C, WHSV: 7 h^{-1}, H_2/HC: 2 mol/mol; data from refs. [27,79]

Table 5, during toluene disproportionation, the resultant *p*-xylene selectivity is higher while using PMS as the impregnation source instead of DMS. Moreover, at similar conversion levels, selectivation by silicon impregnation from PMS is found to retain higher catalyst activity than the pre-coking modification, as shown in Fig. 21. In general, the silica modification method suffers less from lower activity than the pre-coking selectivation technique. The modification by pre-coking method produces higher benzene and gas yield and a higher benzene-to-xylene ratio, which may be due to the higher reaction temperature in this context. Moreover, the silicon modification by PMS tends to provide a stable activity. Overall, the two modification methods both yield a similar line-out *p*-xylene selectivity of ca. 86%, as shown in Fig. 22, however, silica deposition produces lower A_9^+ than pre-coking (Table 4). Sensitivity studies showed that process economics of toluene disproportionation process greatly improves with reducing benzene-to-xylene ratio. So far, the MTPX^{SM} Process has the lowest benzene-to-xylene ratio (Table 4) and best economics [12,121].

In situ silica modification techniques included surface silylation by using silane [107] or chemical vapor deposition method by using organosilicon compounds [122,123], the so-called CVD method. Silica deposition pretreatment can be either a separate procedure or co-feeding with reactants. In the latter case, silicone reagent was co-fed with toluene to modify the catalyst and conduct toluene disproportionation simultaneously. The silicone reagent was discontinued when desired toluene conversion and *p*-xylene selectivity were reached. The technique can be combined with *ex situ* silica impregnation to fine tune zeolite structural features and has been termed "trim selectivation" [118].

Chang et al. [123] found that HMDS (hexamethyldisiloxane) selectivation sustains a better activity retention, at ca. 25% toluene conversion and ca. 88% *p*-xylene selectivity, than the other siloxane modification agents, such as TMDS (1,1,2,2-tetramethyldisiloxane) or PMDS (pentamethyldisiloxane), and TEOS (tetra-ethyl-orthosilicate). TEOS selectivation resulted in a more rapid catalyst deactivation. However, the CVD technique using orthosilicate compounds, with the structure of $SiR_n(OR)_{4-n}$, was successfully applied in EB disproportionation, as discussed below. Niwa et al. [124] pioneered the technique in the modification of the pore structure of mordenite.

Encouraged by the success of MSTDP^{SM} Process and MTPX^{SM} Process, there have been many active research attempts to fine tune selectivation techniques to further improve *para*-isomer selectivity, while also reducing side products and approaching benzene-to-xylene molar ratio of unity. James et al. [30] of UOP (Union Oil Products) reported recently a new toluene disproportionation process, PX-Plus^{SM}, with a high *p*-xylene selectivity of ca. 90% at toluene conversion

level of 30%. It applies an on-line selectivation pretreatment in the start-of-cycle, consisting of three stages, i.e., oil-in at typical operating conditions, a selectivation stage for *para*-isomer selectivity improvement, and then lined out normal operation at enhanced *para*-isomer selectivity. However, the relevant details of their selectivation techniques were not disclosed. The benzene-to-xylene molar ratio of PX-PLUS^{SM} is 1.37, which is close to that observed in MSTDP^{SM} (1.3) (Table 4).

3.4. Effects of para-isomer selectivity on production scheme

As mentioned earlier in Section 3.2, for *p*-xylene recovery, the adsorptive separation method is more favorable than the crystallization method, mainly because the former not only has higher recovery rate but also yields high purity *p*-xylene. Recent advances in *para*-selectivity enhancement, as discussed above, have created a significant impact on the production scheme of high purity *p*-xylene. The concentration of *p*-xylene is found to reach up to 80–90% with MSTDP^{SM} [27], MTPX^{SM} [78,79] and PX-Plus^{SM} [30]. Crystallization processes for various compositions of A_8 aromatics, obtained from different xylene processes with and without thermodynamic equilibrium, are listed in Table 6. As long as the *p*-xylene concentration in A_8 mixtures increases, then temperature of the eutectic mixture decreases, whereas isomer contamination in the *p*-xylene product decreases correspondingly (Fig. 8). There is no requirement for the *p*-xylene enriched mixtures in crystallization to cool down to the eutectic temperature, such as for A_8 mixtures with thermodynamic equilibrium composition, high recovery rate and high quality (99.5%) of *p*-xylene is achieved in a single stage [78]. Typical operating temperatures for the crystallization method are in the range of −20–4°C, with a high recovery rate up to ca. 90%, and hence the production cost decreases substantially (Table 6, Fig. 9).

Table 6
Crystallization processes for various xylene compositions

A_8 component	Mix-xylene production process	
	Thermodynamic equilibrium process[a]	Para selective process[b]
p-Xylene (%)	21	78–90
m-Xylene (%)	48	3–14
o-Xylene (%)	21	1–3
Ethylbenzene (%)	10	5–8
Crystallization process		
Number of stages	2	1
Temperature (°C)	∼−70	∼−20–4
Recovery rate (%)	65	80–90

[a] Produced from A_7 disproportionation and A_9 transalkylation.
[b] Produced from MSTDP^{SM}, MTPX^{SM} and PX-Plus^{SM}.

Advances in the disproportionation process thus revived crystallization technology. Owing to the high recovery rate of *p*-xylene, there is a much less fraction of raffinate stream as compared to the conventional thermodynamic equilibrium mixture. The raffinate stream can be directly charged into an existing adsorption recovery process or combined into conventional xylene mixtures. In addition, a new production scheme producing *p*-xylene only can be designed as a stand alone *p*-xylene complex comprising *p*-xylene selective disproportionation processes (such as MTPX^{SM}) and utilizing the crystallization method for the recovery unit in the absence of a xylene isomerization unit. Such a new production scheme (Fig. 23) is very simple, and should have much lower capital investment cost and minimal, more economic size compared to the conventional *p*-xylene complex (Fig. 7).

According to Mobil Oil, the MTPX^{SM} Process, the latest commercial process, requires an even lower capital investment and operating costs by 10–15% than the MSTDP^{SM} Process [121]. It should further reduce the capital and operating costs compare to the other conventional *p*-xylene processes.

3.5. Development of transalkylation process

The transalkylation process deals with methyl group transfer between toluene and A_9 molecules, which are readily available from catalytic reforming and naphtha cracking. Both the transalkylation process and toluene disproportionation process can convert toluene into xylene and benzene. They are used in most aromatic complexes to increase the *p*-xylene production from catalytic reforming. As shown in Fig. 24, *p*-xylene production was evaluated with various types of BTX complex. They include reforming unit alone (Reforming), reforming plus toluene disproportionation (Ref+TDP) to use up surplus toluene,

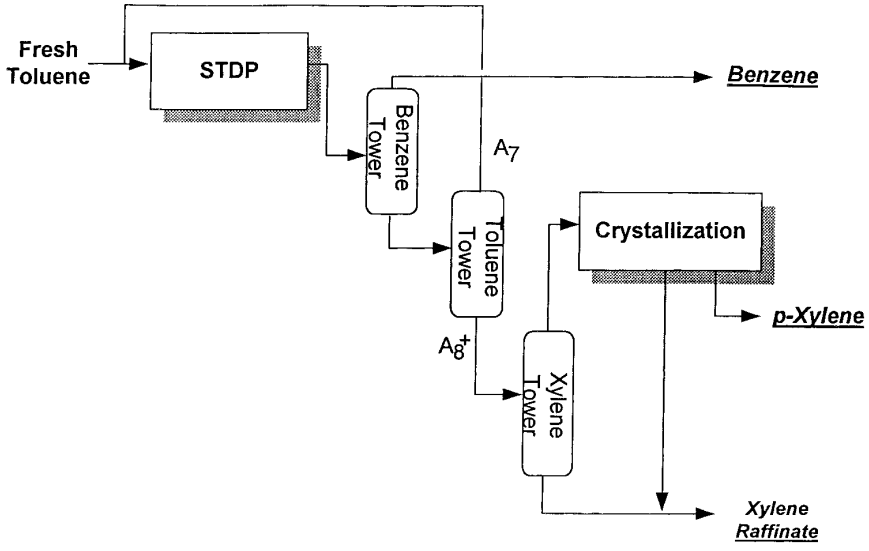

Fig. 23. Simple *p*-xylene production scheme using selective toluene disproportionation processes (STDP) and crystallization recovery technology.

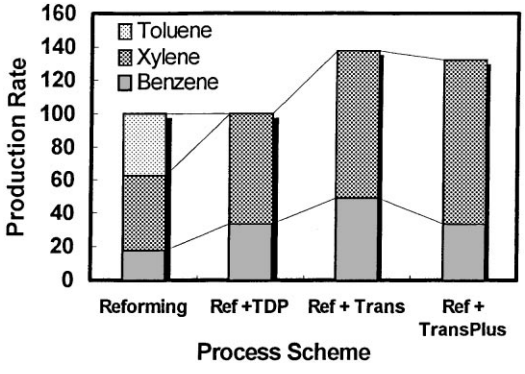

Fig. 24. Comparison of BTX production rate among various process integration schemes by using reforming process as base; data from refs. [3,33,37].

and reforming unit plus transalkylation, either typical transalkylation processes (Ref+Tans) or particularly TransPlus[SM] Process (Ref+TransPlus), by conversion of surplus toluene and additional A_9. In Fig. 24, the BTX production rate of the reforming complex is the base case. By comparison with the base case, the production rates of benzene and xylenes in Ref+TDP complex increase by 88% and 48% respectively; in the transalkylation process scheme, they increase by 88% and 119% for Ref+TransPlus scheme, and by 177% and 96% for Ref+Trans scheme, respectively [3,33,37]. Total feed and BTX production rates remain the same for the former case and increase by around 35% for the transalkylation case. Transalkylation thus boosts more xylene production than disproportionation.

The transalkylation reaction is thermodynamically controlled, where the equilibrium aromatic compositions are mainly dictated by the methyl group per benzene ring (*M*/*R* ratio) of the system, as shown in Fig. 25. For disproportionation of pure toluene feed, the *M*/*R* ratio was unity. In practical operation, *M*/*R* ratio increases with increasing percentage of heavy aromatics, especially A_9 and A_{10}, in the feed composition. By increasing the A_9 blending percentage in toluene feed, xylene yield is enhanced at the expense of benzene yield [125]. Therefore, transalkylation process is more selective for xylene production than toluene disproportionation process. Maximum thermodynamic equilibrium xylene yield was achieved at *M*/*R* ratio of 2. Transalkylation process is thus more attractive to refineries having naphtha-cracking units which produce excessive A_9 products or marketplaces having higher demand for xylene than benzene.

Unlike the toluene disproportionation process, whose performance is commonly characterized by

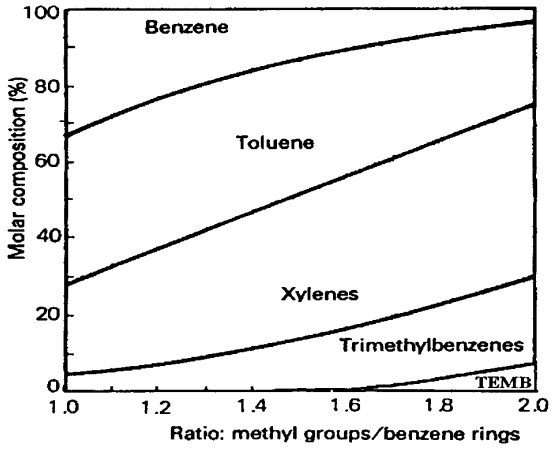

Fig. 25. Plot of equilibrium composition of aromatics varies with the ratio of methyl groups/benzene rings; adaped from refs. [63,125].

the *p*-xylene yield, transalkylation process is normally evaluated by its yield pattern particularly total xylene yield, feed impurities tolerance level, maximum A_9 concentration in feed, cycle length and product purity.

3.5.1. Feed composition effects

A typical A_9 fraction contained ET (methyl-ethylbenzene), TMB and many other compounds [37,126–128], as shown in Table 7. It contains minor compounds, especially propylbenzene, indane, indene and small amounts of A_{10} [126,127]. Because those compounds have boiling points close to TMBs and methylethylbenzenes, they are difficult to separate economically. There were two major issues relating to feed compositional effects. The first issue is the product selectivity of major A_9^+ components and the second issue is catalyst stability or cycle life, particularly the concern arising from minor A_9^+ compounds.

Table 7
Typical compositions of A_9 stream [37,128]

Components	A_9 (%)	A_9^+ (%)
C_8 aromatics isomers	12.9	2.4
C_9 isoparaffins	–	0.2
Isopropylbenzene	1.2	0.4
n-Propylbenzene	3.6	2.7
Ethylmethylbenzene	36.1	19.0
Trimethylbenzene	44.8	30.5
Indane	0.5	1.0
C_{10}^+ aromatics	0.9	43.8
Butylbenzene	–	3.3
Methylpropylbenzene	–	9.5
Diethylbenzene	–	3.5
Dimethylethylbenzene	–	18.2
Tetra-methylbenzene	–	7.8
Methylindane	–	1.5
Total	100.0	100.0

Transalkylation process comprises a complex reaction network, as shown in Fig. 26, which was proposed earlier by many researchers [125,92,129–133]. In transalkylation routes, toluene reacts via a bi-molecular reaction intermediate (biphenylmethane carbenium ion intermediate [125,92]) with TMB to form xylenes (reaction (5)), and with ET to form EB plus xylenes (reaction (6)). In disproportionation routes, TMB produces xylenes and tetramethylbenzenes, reaction (7), whereas ET reaches equilibrium with DEB plus xylenes, reaction (8). ET first dealkylates into toluene and ethylene, reaction (9), following which the former then further reacts via disproportionation, reaction (1), or transalkylation, reactions (5) and (6), the latter further reacts with benzene to form EB, reaction (10). In addition, there are side reactions and all are not limited by thermodynamics, including dealkylation of alkylbenzenes by reaction (11) and ring saturation by reaction (12) or cracking by reaction (13) to form naphthenes or further cracking into gases. In the paring reaction, TMB reaches equilibrium with ET through a 5-membered ring carbocation, reaction (14) [131–133]. The hypothesis of the paring reaction was supported by the formation of ethane and butane in transalkylation products [133].

Dealkylation, by reactions (9), (11) and (15) with formation of toluene and benzene, reduces the *M*/*R* ratio of the whole thermodynamic equilibrium reaction system and is less favorable for xylene yield. It might also reduce apparent toluene conversion. On the other hand, the existence of the paring reaction would cause reequilibration and affect conversion levels of individual A_9 compounds. Increased A_9 feed content is favorable for xylene production. However, as shown in Fig. 27, EB content in A_8 mixtures increases as *M*/*R* ratio increases [134], which deteriorates xylene quality and increases *p*-xylene recovery cost. Das et al. [129,135] studied the product yields of transalkylation between toluene and three TMB isomers and *o*-ET. With similar feed at toluene-to-A_9 compounds ratio in

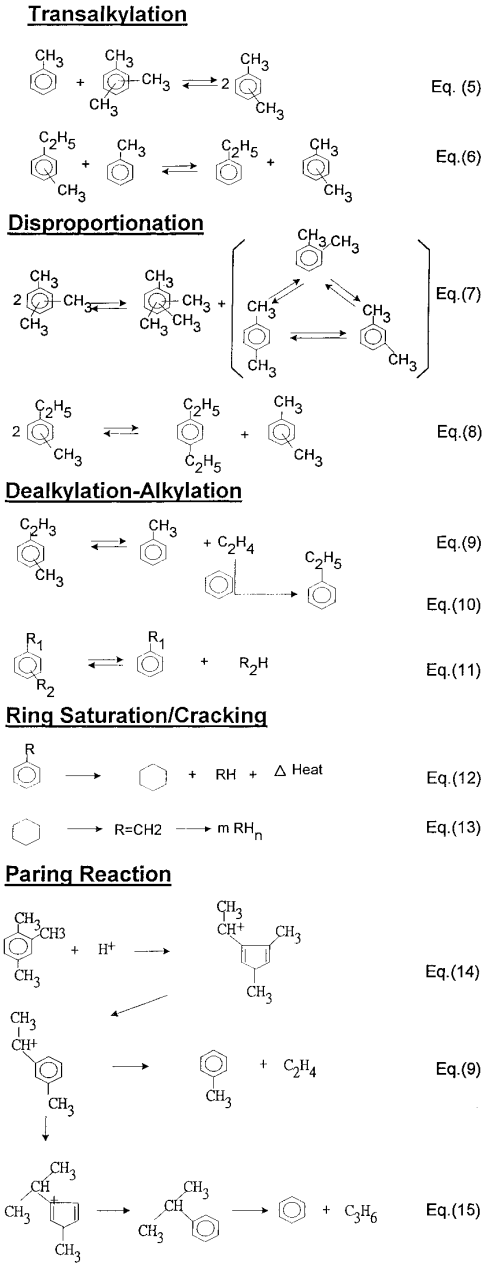

Fig. 26. Transalkylation reaction network.

the vicinity of 50:50, EB selectivity in A_8 was 43% for *o*-ET feed, in comparison to c.a. 0.2–2.5% for TMB feed. Among the three TMB isomers the A_9 feed 1,2,3-TMB gave the highest EB yield. Accordingly, EB formation can be attributed to transalkylation of ET by

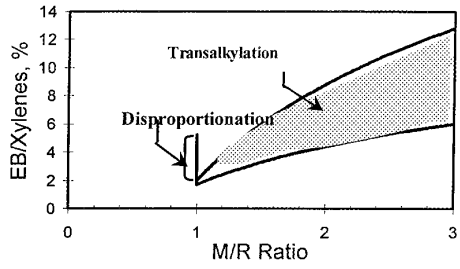

Fig. 27. Ethylbenzene content in xylene mixtures of various disproportionation processes and transalkylation processes.

reaction (6) and dealkylation/re-alkylation by reactions (9), (10) and (11). The paring reaction of TMB to form ET, reaction (14), contributes additional EB yield.

3.5.2. Catalyst stability

Catalyst stability is one of the main issues in process development. Wang et al. [125] reported that zeolite Beta is stable in the disproportionation of TMB without the presence of hydrogen, while mordenite and USY deactivate seriously. Their work demonstrated the potential of zeolite Beta in transalkylation process.

Absil et al. [136] investigated transalkylation of toluene and A_9^+ aromatics for a wide range of compositions over various zeolites. The A_9^+ aromatics test feed contained 14.4% C_{10} aromatics. Different test feeds with toluene-to-C_9^+ ratios of 60/40 and 100/0 and one other feed which contained 10 wt% *n*-decene, a non-aromatic, were investigated. As shown in Table 8, for the three types of zeolites (which all contain platinum) the xylene-to-benzene ratio increases with increasing C_9^+ feed percentage, which is guided by thermodynamic equilibrium. Zeolite Beta showed the greatest transalkylation activity as indicated by the greater xylene-to-benzene ratio. On the other hand, the MCM-22 without platinum produced an almost equal molar mixture of xylene and benzene. In terms of xylene-to-benzene ratio, Pt–Zeolite Beta was the greatest one with a 40% A_9^+ feed (Feed A) while Pt–ZSM-12 was the top one with 100% A_9^+ feed (Feed B). It was also found that Pt–ZSM-12 and Pt–mordenite are more favorable for the conversion of ET than TMB. In contrast, Pt–zeolite Beta is more favorable for TMB conversion with toluene-rich feed and more favorable for ET conversion with pure C_9^+ feed. More-

Table 8
Transalkylation results over various zeolites [136]

Zeolites	Pt–Beta[a,b]			Pt–Mordenite[a,b]			Pt–ZSM-12[a,b]			MCM-22[c]
	A	B	C	A	B	C	A	B	C	
Feed (wt%)										–
Toluene	60	0	0	60	0	0	60	0	0	67.5
C_9^+ aromatics	40	100	90	40	100	90	40	100	90	32.5
n-Decene	0	0	10	0	0	10	0	0	10	0
Conversion (wt%)										
Trimethylbenzene	62	44	21	57	40	34	54	52	34	–
Ethylmethylbenzene	55	66	42	68	66	56	70	77	68	–
C_{10} aromatics	37	<1	–	49	31	9	39	31	17	–
C_9^+ aromatics	–	–	–	–	–	–	–	–	–	66.5
Xylene/benzene (mol)	2.86	5.88	2.86	1.96	5.26	4.55	1.79	6.67	5.88	1.02

[a] Pt content: 0.1 wt%.
[b] Reaction conditions: 427°C, 1825 kpa, WHSV 2 h^{-1}, H_2/HC 2 mol/mol, 48 h on stream.
[c] Reaction conditions: 474°C, 42.3 kg/cm^2, H_2/HC 2 mol/mol, WHSV 4 h^{-1}.

over, Pt–ZSM-12 exhibited the greatest activity with pure C_9^+ feed (Feed B) and it also demonstrated the greatest tolerance towards decene poisoning. Both Pt–ZSM-12 and Pt–mordenite showed higher A_{10} conversion than Pt–zeolite Beta.

The incorporation of metal onto the zeolite catalyst was mainly to enhance the operation cycle length [137]. For example, Shamshoum et al. [138] applied nickel at 1.4% to improve the stability of mordenite in A_9 transalkylation, which allowed a tolerance for 13% A_9 in the feed at a deactivation rate below 1.4°C/day. However, as a result of metal incorporation, a substantial increase in undesirable aromatics saturation side reactions. This is because hydrocracking of alkylbenzenes and aromatic saturation cause the formation of non-aromatics, which results in loss of aromatics yield, excessive heat of reaction and, most seriously, deterioration of product quality. In particular, benzene saturation generates the formation of cyclohexane and methylcyclopentane, reaction (12), which both have boiling points close to that of benzene. Their presence not only increases the freezing point, but also down grades the quality of the benzene product. The effect is normally expressed as ring loss [139]. Buchanan et al. [140] had applied an on-line sulfiding technique to reduce the ring loss. Shamshoum et al. [141] reported that aromatics saturation and non-aromatics formation over Ni(1%)-mordenite can be suppressed by reducing the H_2-to-aromatics ratio temporarily in the start-up period. Therefore, the excessive ring loss and reaction exotherm can be prevented during the start-up period. The line out H_2-to-aromatics ratio was raised by the end of the start-up period, i.e., one month, to extend catalyst cycle length. However, no matter with the start-up procedures, ring loss was mainly dependent on H_2-to-aromatics ratio at line-out operating conditions.

3.5.3. Commercial transalkylation processes

A summary of commercial transalkylation processes is shown in Table 9. It is noted that all of them utilize large-pore zeolite catalysts, with constraint index from 1 to ca. 3 [23], to favor greater diffusivity of A_9 molecules inside the zeolite pore. It was reported that ZSM-5 can process A_9 up to 25% [73]. However, pore of ZSM-5 (5.6Å) was too small for most A_9 molecules, which have critical dimensions around 7.6 Å [142]. By calculation on the experimental results over ZSM-5 reported by Meshram et al. [130], conversion of ET and TMB was around 84% and 40%, respectively. Recently, O'Connor et al. [143] reported that isomerization of 1,2,4- and 1,3,5-TMB occurred on external sites of ZSM-5. Therefore, ZSM-5 more selectively converted ET rather than TMB. The unconverted A_9 will be rich in TMB. In practical operation, A_9 is used in once through mode to prevent

Table 9
Summary of commercial transalkylation processes

	Process name		
	Xylene-plus[a]	Tatoray[b]	TransPlus[c]
Developer	ARCO–IFP	UOP	Mobil–CPC
Feedstock	A_7+A_9	A_7+A_9	$A_6 + A_9^+/A_7 + A_9^+$
Maximum A_9 content (%)	~15 (Normal)	40	100
A_{10} content in A_9^+ (%)	Limited	Limited	10–25
Catalyst identification	EMCAT	TA-4	TransPlus
Reaction conditions			
Reactor type	Moving bed	Fixed bed	Fixed bed
Temperature (°C)	454–538	380–500	385–500
Pressure (kg/cm^2)	1.1–l.3	29.6–40.1	21–28
H_2/HC (mol)	None	4–6	1–3
Catalyst/oil ratio (wt/wt)	1–2	None	None
WHSV (h^{-1})	0.7–1.7	1.5–2.2	2.5–3.5
Conversion (wt%)	30–45	40–50	45–50
Xylene/benzene ratio (mol)	1–1.5	1.1–2.5	1.1–10.1
Cycle length (years)	Continuous catalyst make-up	>2	>2

[a] Refs. [54,63,134].
[b] Refs. [32–34].
[c] Refs. [35–37].

accumulation of TMB in the recycle A_9 stream. The preference in conversion for ET over TMB was also observed over Pt–ZSM-12 and Pt–mordenite, but not Pt–zeolite Beta (Table 8), and can be attributed to pore opening size effects.

The Xylene-Plus^{SM} is the only process that applies the continuous circulation reactor design similar to the earlier TCC (Thermofor Catalytic Cracking) Unit. Both designs contained a reactor and a regenerator in which catalyst was subjected to regeneration continuously and circulating back to the reactor to deal with the serious catalyst deactivation problem. It applies a faujasite based catalyst [144]. The circulation rate of the catalyst can be either measured from the pressure difference in the lift pipes or calculated by heat balance [134]. Thus, the unit operates at a much higher reaction temperature, typically in the range of 450–540°C, and is energy intensive as compared to the other process types [63]. In the Xylene-Plus unit, the contact time of the reaction was controlled both by catalyst-to-oil ratio and the space velocity (WHSV). As a result, the operation is much more complicated compared to the fixed bed reactor system, in which the contact time is solely determined by WHSV.

Due to the existence of impurities in the A_9 feed, the cycle life of the catalyst is a major concern in fixed bed reactor processes. This is, of course, in contrast to the continuous regeneration scheme used in Xylene-Plus^{SM} process. There are two types of fixed bed transalkylation processes; the Tatoray^{SM} Process was developed by UOP and the TransPlus^{SM} Process was jointly developed by Mobil Oil and Chinese Petroleum. Fixed bed transalkylation processes generally have higher liquid yield than the moving bed process.

A generic process flow diagram is presented in Fig. 28. Toluene plus C_9^+ feed and hydrogen (including both recycle and make-up) pass through zeolite catalyst bed of reactor. Benzene, xylene and A_{10}^+ heavy aromatics products then are separated in the top of the benzene tower, xylene tower and A_9 tower; toluene and A_9^+ are separated from the top of the toluene tower and heavy aromatics tower and recycled for extinction conversion. Hydrogen is recycled through a recycle compressor. Process flow of the disproportionation processes discussed above is exactly the same, but without the A_9 tower and A_9^+ recycle stream.

As discussed earlier, transalkylation reactions were controlled by thermodynamics. In accordance with

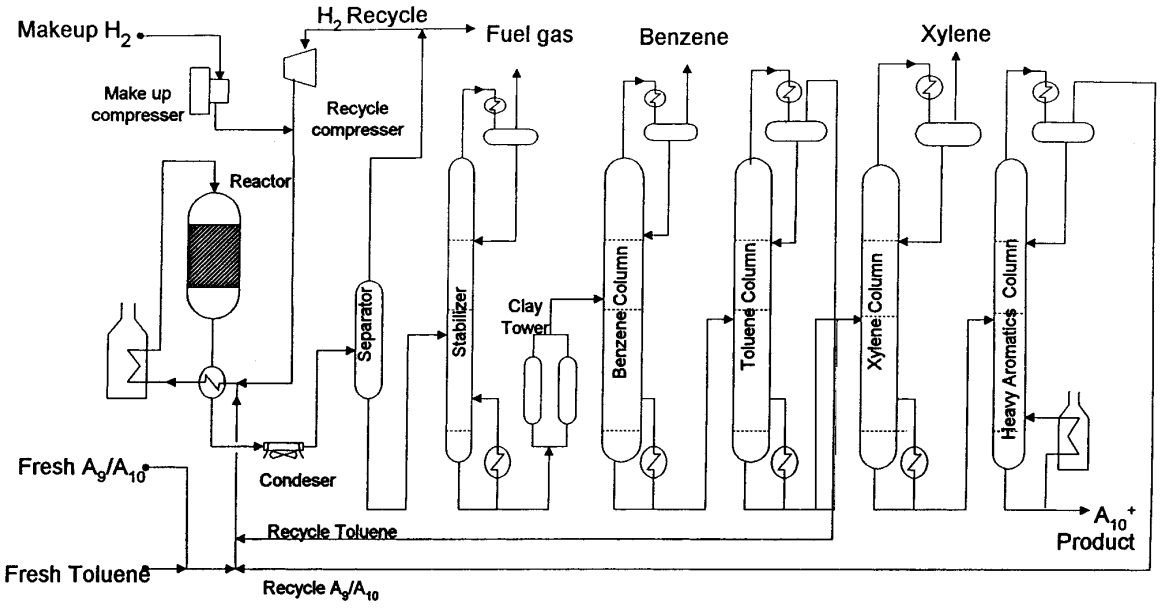

Fig. 28. Generic process flow scheme of transalkylation; modified from refs. [37,63].

thermodynamics, xylene yield increases and xylene-to-benzene ratio increases with increasing A_9^+ feed content. In addition, there are a lot of A_9 cracking reactions to light gases, reactions (11) and (12), leading to liquid yield loss and more A_{10} yield by A_9 disproportionation. Although it is desirable to increase A_9^+ feed content, there is an economic trade-off. As A_9^+ price is usually lower than BTX aromatics [33], increasing A_9^+ feed content can reduce transalkylation feed cost.

As long as the *M*/*R* ratio of feed is the same, the product yields of various processes are similar. In considering process characteristics, the major differences among them were:

1. operable A_9^+ feed content, including feed specification and cycle length,
2. liquid yields, including maximum xylene yield, and
3. product quality, including EB yield, product purity.

Each process has its characteristic constraints in the maximum achievable A_9 feed percentage. The XylenePlus^{SM} Process, when processing high A_9 feed, had mechanical issues, particularly coke combustion capacity and regenerator metallurgy, plus the added concern of deterioration of benzene product purity. It was claimed that the XylenePlus^{SM} Process is capable of processing a feed with more than 90% A_9 [54]. However, high A_9 feed operation needs to cope with the above-mentioned concerns. In practical operation, A_9 feed content in XylenePlus^{SM} operation is 0–15% [134].

In general, the transalkylation process has a strict feed specification, for example, contents of indane and A_{10} are required to be low in order to sustain a long cycle length. It was reported that the TransPlus^{SM} Process can accommodate up to 25% of A_{10} in the A_9^+ feed [36,37]. With a thermodynamically controlled system, A_{10} in feed would suppress the A_{10} yield by disproportionation of A_9. This is a useful technique to ease the counter drawback in processing high A_9 feed. Since A_{10} price is low even relative to A_9, the excessive A_{10} feed can reduce feed cost and significantly strengthen process economic. The A_{10}^+ content can be adjusted via the cut point of A_9^+ tower operation. This is the first fixed bed commercial transalkylation process that is capable of handling excessive A_{10} feed. It has been shown that even with a moderate increase in the tolerance to feed impurities, the cycle length of the TransPlus^{SM} Process was longer than two years [36,37]. The relaxed feed spe-

cification therefore, expands the supply of feed sources to accommodate more throughput and thus makes the process more attractive. There is wide flexibility to adjust product yields with xylene-to-benzene molar ratio in the range of ca. 1.1–10.1, in comparison with other transalkylation processes which operate in the range of ca. 1.1–2.5 (Table 9).

EB content in A_8 mixtures is of concern of *p*-xylene recovery in the adsorption process. EB contents in A_8 mixtures produced from reformate and pyrolysis gasoline are around 10–15% and 15–33%, respectively. As shown in Fig. 27, both transalkylation and disproportionation produced high quality xylenes with EB content is well below 8%. They are the most favorable xylene sources for *p*-xylene recovery units. All toluene disproportionation processes produced xylenes with an EB selectivity of 2–3%, no matter what the improvement in *para* selective processes. For the xylenes produced by transalkylation, EB content changed with *M*/*R* ratio of feed. The drawback of increasing EB content should be taken into account. It could exert a limitation to the maximum A_9 feed composition in some cases with limited adsorption recovery capacities. There were differences among various transalkylation processes. A moving bed reactor applied a much higher reaction temperature (Table 9), at which re-ethylation of benzene was slower than the de-ethylation of ET, thus producing a lower EB content. Interestingly, the TransPlus[SM] Process produced low EB content, ca. 2.7%, even at 100% A_9^+ feed [37].

Table 10
Feed and product slates of TransPlus[SM] Process [37]

Product mode	Benzene/ xylene	Benzene/ xylene	Toluene/ xylene
Feed (wt%)			
Toluene	60	0	0
Benzene	0	0	25
A_9+A_{10}	40	100	75
Product yields based on converted feed (wt%)			
C_5^- gas	5.2	18.5	9.2
Benzene	20.6	3.4	–
Toluene	–	22.9	39.8
Ethylbenzene	2.7	1.3	2.3
Mixed xylenes	64.3	46.5	40.6
Heavy aromatics	7.2	7.4	8.1
Total	100	100	100

In addition to the conventional mode with benzene and xylene as product slate and toluene and A_9^+ as feed, TransPlus[SM] Process also provided another operation mode, i.e., as toluene and xylenes product slate, by converting benzene and A_9^+ feed under similar operating conditions (Table 10). The xylene-to-toluene product distribution can be altered by manipulating the feed compositions of benzene-to-A_9^+. Feed source and product slate between benzene and toluene are interchangeable in accordance with the price differential among aromatics. The wide range spectrum in feed selection and product slates offers flexibility and economic incentives in response to market fluctuations to maximize process profits. Benzene feed mode can be useful particularly due to more stringent limitation regulation of benzene in RFG.

4. *p*-Diethylbenzene production

4.1. p-Diethylbenzene market

p-Diethylbenzene (*p*-DEB) has a much higher product value (ca. US$ 4000 per metric ton) than *p*-xylene (ca. US$ 450 per metric ton). It is used as desorbent in adsorptive separation processes, for example, in Parex[SM] (UOP) and possibly also in Eluxyl[SM] (IFP) [4,54,55]. There is a constant demand for the routine make-up requirements of existing operating units, with estimated consumption of 8000 tons/year. In addition, there are requirements for new loads of *p*-DEB for grass root units, with estimated demand of around 4000 tons/year. Therefore, worldwide annual demand is estimated as 12 000 tons, accounting for annual sales volume around US$ 48 million dollars.

4.2. Development of selective ethylbenzene disproportionation process

In past production scheme, *p*-DEB was mainly recovered from the DEB mixtures that are normally multialkylation side products of the EB process. Three DEB isomers exist, namely, *p*-, *m*- and *o*-DEB, all of which have very similar physical properties (Table 2). For example, the boiling point and melting point of

p-DEB and *o*-DEB only differ by 0.3°C and 11.7°C, respectively. Although it has not been disclosed, it is generally believed that the early *p*-DEB recovery was mostly done by adsorptive separation. There are several drawbacks for applying adsorptive separation for *p*-DEB recovery. The technique is energy intensive. Moreover, owing to the distribution of EB production, the feed (DEB) has to be collected from different manufacturers and thus increase the feed collection cost. Furthermore, the separation raffinate (mainly *m*- and *o*-DEB isomer mixture) can only be used as fuel oil and the mixed DEB feedstock required to produce one pound *p*-DEB is ca. 4 pounds. These three factors, namely, high energy consumption for separation, high feed collection cost and high feedstock requirement, are the main reasons that made the *p*-DEB cost high.

DEB can also be produced by the EB disproportionation reaction, which the R in reaction (1) stands for ethyl group. A variety of different zeolitic catalysts, such as ZSM-5, mordenite, faujasite and zeolite Beta, etc. have been studied [145–147]. Compared to other monoalkylbenzene processes, EB disproportionation has a much more stable activity [147]. Most catalysts show acceptable stability in EB disproportionation. The products obtained in the disproportionation reaction normally give the thermodynamic equilibrium composition that requires energy intensive operation for *p*-DEB recovery. Thus, the technical challenge in producing *p*-DEB by EB disproportionation is technology development to enhance *para* selectivity. In line with the developments in *para* selective processes, discussed earlier, many earlier approaches are applied for *p*-DEB process development.

Wang et al. [22,31,122] applied an *in situ* surface silylation by chemical vapor deposition (CVD) method to modify ZSM-5, by which they were able to obtain *p*-DEB with product selectivity up to 99%

Table 11
Temperature requirement of Si–CVD deposition for various substrates [22]

Substrates	Deposition temperature (°C)
H–ZSM-5	<180
SiO_2–Al_2O_3	<180
Al_2O_3	~230
Kieselguhr	>320

$P_{Si(OC_2H_5)4}$: 2×10^3 pa, residence time: 5 s, conversion: 50%.

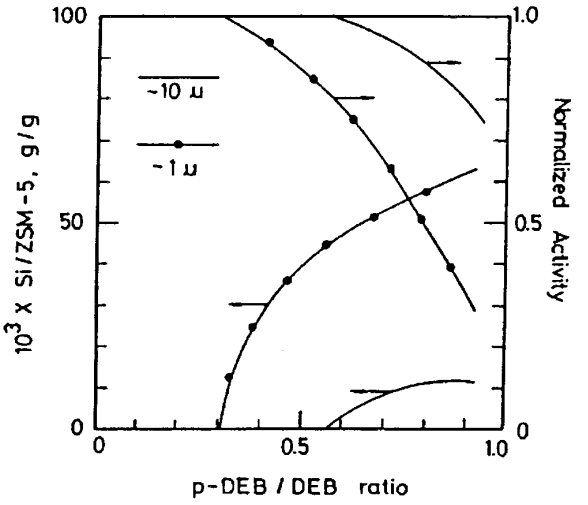

Fig. 29. Effects of silica deposition concentration and *p*-DEB selectivity and normalized activity; reaction conditions: reaction temperature: 340–390°C, ethylbenzene WHSV: 3.5 h^{-1}; reproduced from ref. [22].

directly from EB disproportionation. They used orthosilicate mixture as the modification agent; typical composition of the selectivation mixtures was 45% methanol, 50% EB and 5% TEOS. Selectivation procedure was conducted at the temperature shown in Table 11 until orthosilicate breakthrough was observed. The authors disclosed that orthosilicate first adsorbed on the external sites of the zeolite and then hydrolyzed into silica on the substrate. The hydrolysis temperatures vary with the type of substrate, as shown in Table 11. For example, ZSM-5 requires a lower hydrolysis temperature, ca. <180°C, compared to the other substrates which are less acidic (for example, kieselghur). The authors also concluded that, among the various types of orthosilicates investigated, silylation by tetraethyl-orthosilicate (TEOS) yielded the best *p*-DEB selectivity. Moreover, the crystallite size of the zeolite and the extent of SiO_2 deposition are also found to play an important role on selectivation performance, as shown in Fig. 29. For example, for a large crystalline sample of 10 μm, only 1.1 wt% of silica deposition is required to achieve *p*-DEB with 99.4% purity and the composition so-produced maintained 80% of initial activity. In contrast, for substrate crystalline size of 1 μm, a silica content of 6.4 wt% is required to achieve the same *p*-DEB selectivity and the

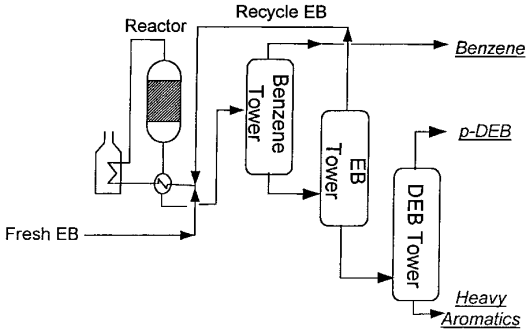

Fig. 30. Flow diagram of *p*-DEB manufacturing process; courtesy of Taiwan Styrene Monomer.

Table 12
Representative properties of *p*-DEB products by Taiwan Styrene Monomer

Trade name	TSD-980	TSD-990
Purity (wt%)	98.4	99.1
C_9 aromatics and lighter (wt%)	0.07	0.05
Other C_{10} aromatics (wt%)	1.17	0.75
C_{11} aromatics (wt%)	0.40	0.10
Total S (wppm)	Nil	Nil
Total nitrogen (wppm)	0.35	0.22
Total chloride (wppm)	Nil	Nil
Carbonyl number (mg/l)	1.5	0.14
Bromine index (mg/100 g)	0.89	0.56
Color, APHA	5	3
Specific gravity (g/cc at 4°C)	0.863	0.863

composition retains lower initial activity down to 30%. Zeolite catalysts with a larger crystalline size therefore require a small amount of deposited SiO_2 to achieve high *p*-DEB selectivity and, more importantly, to retain a better activity. These observations are consistent with results of *p*-xylene selectivity in toluene disproportionation reported by Haag and Olson [91] (Fig. 12).

The above *p*-DEB selectivation process using modified ZSM-5 by Si–CVD surface silylation method was successfully commercialized by TSMC in 1988. The commercial plant that produced *p*-DEB with 96% purity began its operation in 1990 with an annual production capacity of ca. 4000 tons/year. A schematic flow diagram of the process is depicted in Fig. 30. Recently, TSMC further upgraded their *p*-DEB production purity to 99%; representative analysis resulted into two commercial grade products are shown in Table 12. The TSMC process has a cycle length of over six months and its catalyst is fully regenerable.

The *para* selectivity of various alkylbenzenes over modified catalysts by Si–CVD deposition has also been investigated by Wang et al. [87]. Based on the results summarized in Table 13, the *para* selectivities are the same for *p*-DEB products obtained from either disproportionation or ethylation of EB, whereas *p*-ethyl-methylbenzene (*p*-ethyltoluene, *p*-ET) selectivies obtained from toluene transalkylation with EB and toluene ethylation are nearly the same. However, the observed *p*-xylene selectivity by methylation (ca. 70%) is much higher than that of toluene disproportionation (ca. 55%). Thus, the demand for modification to achieve same *para* selectivity enhancement for alkylbenzenes follows the trend:

$$p\text{-Xylene} > p\text{-DEB} \geqq p\text{-ET}$$

Kaeding et al. [148] reported that MgO can enhance *p*-DEB selectivity up to 99.9% and also suppress formation of other heavy aromatics, such as ET, in the ethylation of EB. Wang et al. [87] compared the *p*-ET selectivity obtained from zeolites modified by

Table 13
Summary of *para* selective reactions [87]

Reaction	Temperature (°C)	*p*-X/X	*p*-ET/ET	*p*-DEB/DEB
2T→X+B	450–550	~55	–	–
T+MeOH→X+H_2O	400–450	~70	–	–
2EB→DEB+B	320–360	–	–	~92
EB+E→DEB	320–360	–	–	~92
T+E→ET	350–400	–	~99	–
T+3EB→ET+DEB	320–360	–	~98	~92

Abbreviations: B: Benzene; DEB: Diethylbenzene; E: Ethylene; EB: Ethylbenzene; ET: Ethylmethylbenzene; T: Toluene; X: Xylene.

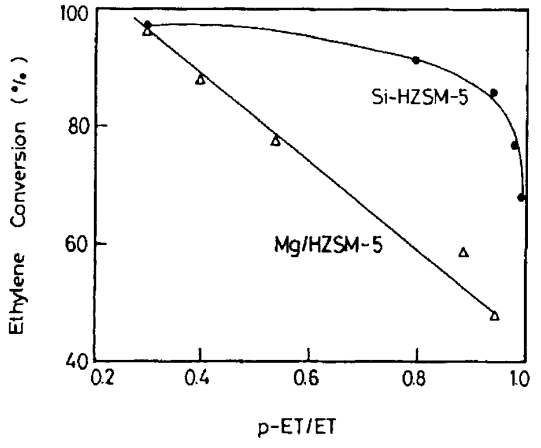

Fig. 31. Comparisons of Si–CVD deposition and MgO impregnation methods of their ethylene conversion and *p*-Methylethylbenzene selectivity in ethylation of toluene; reaction conditions: reaction temperature: 350°C, ethylene WHSV: 0.41–0.58 h^{-1}, toluene/ethylene: 8.8–9.8 mol/mol; reproduced from ref. [87].

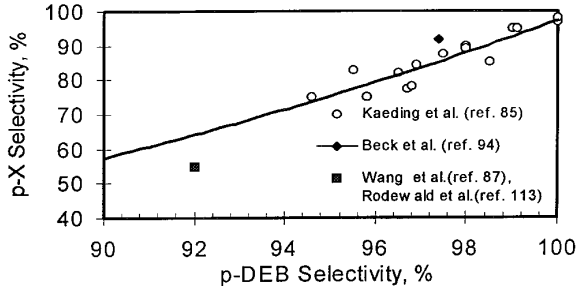

Fig. 32. Correlation of *para* selectivity between disproportionation reactions of toluene and ethylbenzene; data from refs. [85,87,94,113].

Si–CVD deposition with that by magnesium oxide (MgO) impregnation. As shown in Fig. 31, at about the same level of *p*-ET selectivity, ethylene conversion over Si–CVD modified ZSM-5 remains higher than that obtained with MgO impregnation, indicating that the catalyst modification by Si–CVD is more capable of sustaining its activity. It was found that a slight surface modification of the catalyst by Si–CVD is sufficient to enhance *p*-ET selectivity and a substantial loss in conversion occurs only at *p*-ET selectivity beyond ca. 80%. In contrast, conversion dropped almost linearly with *p*-ET selectivity enhancement by MgO impregnation. The diffusivity ratio of *p*-ET to *o*-ET (D_p/D_o) increases by 1.6 times over the Si–CVD modified sample and 9.9 times over MgO-modified sample, while the improvement of *p*-ET selectivity for the former is 99%, and for the latter is 87%, respectively. Therefore, there is no direct relationship between diffusivity and *para* selectivity of ET. The authors proposed that the *para*-isomer is the primary product inside the zeolite channels. The original pore mouth is small enough to allow only *para*-isomer diffuse out and the *para*-isomer selectivity is reduced by the occurrence of fast isomerization on the external surface. Therefore inactivation of the external surface is the major controlling factor for *p*-ET enhancement. This is somewhat contradictory to conclusions made by Haag and Olson [91] for *p*-xylene selectivity enhancement, which requires a substantial catalyst modification in favor of diffusivity (Fig. 12).

A number of authors [85,87,116] have compared the *para* selectivity of various reactions, and their results are summarized in Fig. 32. It is clearly shown that over the same modified zeolite samples, *p*-DEB selectivity is always higher than *p*-xylene selectivity, and almost equally high *para* selectivity was observed only at ca. 99%, which required a very high extent of modification. This obervation can be attributed to the sizes and structures of reaction products. Fang et al. [105] observed that pre-coking pretreatment laid down coke on the external surface and gave *p*-xylene selectivity in the range of 50%. As shown in Fig. 12 [91], diffusion time increased by less than two orders of magnitude to reach 50% *p*-xylene selectivity but had to increase by three orders of magnitude to achieve 80% *p*-xylene selectivity. One hypothesis is that impact of selectivation varies with the extent of modification and has different effects on various reactions. A light and moderate extent of selectivation (which mostly inactivates external surface sites and only little affects on pore opening sizes) enhances *para* selectivity more significantly for larger molecules, such as *p*-DEB, than for small molecules, such as *p*-xylene. A severe extent of selectivation, which reduces pore opening, gives *para* selectivity enhancement to all molecular sizes.

In term of performance over extended operation cycles, Si–CVD modified ZSM-5 is also better than

Table 14
p-DEB manufacturing process by Indian Petrochemical [149]

Parameters	Range
Reactant	Ethylbenzene+ethylene
Reaction temperature	325–375°C
WHSV	1.5–2.0 h^{-1}
EB conversion per pass	10–12%
Cycle length	Over four months
p-DEB selectivity	96–99%

catalysts prepared by MgO impregnation. For example, after catalyst regeneration, the *p*-ET selectivity for the former was maintained at ca. 99.4%, whereas the *para* selectivity for the latter declined from ca. 73% to 67%. Thus, the Si–CVD modification method is more favorable for *para* selectivity enhancement than the MgO impregnation method.

Recently, a few *p*-DEB processes utilizing the selective EB ethylation reaction scheme have also been developed. For example, Halgeri et al. [149] reported a new process that was developed by Indian Petrochemical, which utilized a modified ZSM-5 catalyst. The fully regenerable catalyst has a cycle length of over four months and the *p*-DEB purity increased with day-on-stream from 96% up to 99% at the end of cycle. The profile of the process is presented in Table 14.

4.3. Effects of para-isomer selectivity on the production scheme

The *p*-DEB production scheme has improved drastically after the successful development of *para* enhancement by Si–CVD silylation, which greatly simplifies the production scheme. Compared to the conventional scheme, which was commonly done by adsorptive separation from the mixtures of thermodynamic equilibrium compositions, the new innovated scheme only requires a benzene tower to recover benzene and a separation tower to purify *p*-DEB from C_{10}^{+} heavy aromatics (Fig. 30). Moreover, the new scheme also has a very low flow rate of raffinate which can be disposed as fuel oil or recycle to the benzene ethylation unit. As a result, the state-of-the-art *p*-DEB production plant not only significantly reduces the production cost of *p*-DEB, it is also more friendly to the environment due to its low production rate of by-products.

4.4. Transalkylation of benzene and poly-ethylbenzene

EB is mainly produced from benzene ethylation in the modern petrochemical industry which also produces poly-ethylbenzene co-products. Solid acid catalysts, such as ZSM-5 in the Mobil–Badger EB Process^{SM}, are commonly used. Owing to their shape selective characteristic, zeolitic catalysts, such as ZSM-5, are more effective in inhibiting multi-alkylation product yields compared to the traditional $AlCl_3$ catalyst [7]. EB processes typically contain a transalkylation reactor to improve economic value. Typically, the transalkylation reactor is a smaller reactor other than the main alkylation reactor. The recycled multi-alkylation by-products can then be converted in the transalkylation reactor by the reaction with benzene to EB, and thus enhance the overall production yield. In contrast to the *p*-DEB process, however, the key criteria in the transalkylation process are activity and stability, rather than *para* selectivity. The typical transalkylation process is conducted over a zeolite catalyst at 425–450°C.

5. Diisopropylbenzene production

5.1. Diisopropylbenzene market

Diisopropylbenzenes (DIPB) are useful intermediates for peroxide, resorcinol, hydroquinone and high performance polymers (Fig. 1). In contrast to some of the xylene and diethylbenzene isomers, both *m*- and *p*-DIPB are very useful. Since DIPB has skeletal tertiary carbons, tertiary peroxide radical (dihydroperoxides) can be generated via oxidation, and these are commonly used as initiators for various free radical reactions [150]. The *m*- and *p*-dihydroperoxides can produce resorcinol and hydroquinone plus acetone respectively by rearrangement reaction [151,152].

DIPB can form diisopropenylbenzene by dehydrogenation over Fe_2O_3 in the temperature range of 600°C and 650°C or by oxydehydrogenation with Al_2O_3 [153]. The potential applications of diisopropenylbenzene have been reviewed by Colvin et al. [5],

and include, for example, in engineering plastics, elastomers, films and resins. Diisopropenylbenzene not only has a more versatile molecular structure than divinylbenzene but also a far more interesting chemistry for producing high performance polymers. Moreover, Diisopropenylbenzene is also easier to handle than divinylbenzene. In the absence of acid, Diisopropenylbenzene can be stored as a highly concentrated solution (>99%) without any concern for explosion. Interesting derivatives include high glass-transition temperature polymer (T_g as 280–290°C) [154], bisphenol A derivatives used as flame retardant polycarbonates [155], monoisocynate derivatives used as water soluble polymer [156], and diamine derivatives useful for curing epoxy resins [157], etc.

The number of dialkylbenzene isomer increases substantially as the number of alkyl group carbons increases beyond three. For example, dipropylbenzenes (DPB) have nine isomers as compared to xylene or DEB, which both have three isomers. DPB has three *skeletal* isomers, namely diisopropylbenzene (DIPB), *n*-propylisopropylbenzene (NIPB) and di-*n*-propylbenzene (DNPB), which differ by the branching of the propyl group. Each of the three *skeletal* isomers can further divided into three ring *positional* (*p*-, *m*- and *o*-) isomers. Reactivity and stability of alkyl radicals and carbenium ions vary significantly with the structural arrangement of its carbons, with the order of stability being tertiary > secondary > primary carbon [158]. Therefore, reactivity of *skeletal* isomers are distinctly different. The recovery and purification of *skeletal* isomers are rather complicated, and dedicated distillation, crystallization procedures and adsorption methods are involved. The selectivity enhancement of *skeletal* isomer formation by means of shape selective processes, therefore can substantially reduce the purification cost.

As discussed earlier, selectivity enhancement of ring *positional* isomer formation is the criterion involved in processes which produce *p*-xylene and *p*-DEB. In contrast, selectivity for *skeletal* isomers is the key criterion for DIPB production process.

5.2. Selectivity of diisopropylbenzene in cumene disproportionation

Early production technology for DIPB utilized liquid phase Friedel–Craft catalyst to catalyze cumene (IPB) isopropylation [159]. Depending on the conversion level, the production ratios for *p*-, *m*- and *o*-DIPB isomers may vary from 64:31:5 to 37:60:3. In general, *p*-DIPB is favored at low conversion level whereas the selectivity of the *o*-isomer remains almost unchanged regardless of the operating conditions.

Table 15
Cumene disproportionation over ZSM-12 [163]

	Run number		
	1	2	3
Temperature (°C)	150	200	250
Conversion (wt%)	2.9	13.2	45.1
Product selectivity (wt%)			
Benzene	36.5	33.6	34.2
Diisopropylbenzene (DIPB)	23.8	59.2	60.9
n-Propylbenzene	4.1	0.7	0.7
Others	35.6	6.5	4.2
Benzene/DIPB (molar)	3.19	1.18	1.17
DIPB isomer distribution (%)			
Para	60.5	45.5	35.3
Meta	39.5	53.3	63.9
Ortho	0	1.2	0.8

Recently, there is a trend toward replacing liquid Fridel–Craft catalysts with zeolitic solid acid catalysts for the DIPB production process mainly due to the inevitable corrosion problems and environmental concerns that arise in the conventional processes [160,161]. IPB disproportionation, reaction (16), can be effectively catalyzed only by large-pore zeolites with pore openings larger than 10-membered oxygen rings [147,162]. Kaeding et al. [163–165] reported that ZSM-12 could be used to selectively produce *p*-DIPB. ZSM-12 is a 12-membered oxygen ring zeolite with pore opening of 5.5×5.9 Å [39]. IPB disproportionation reactions are usually carried out at relatively low temperatures (150–250°C). As shown in Table 15, high benzene-to-DIPB product molar ratio and high levels of propylene oligomers were observed at a reaction temperature below the boiling point of PB such as 150°C, indicating the preference of dealkylation reactions. A significant amount (4.1%) of *n*-propylbenze was also observed, which can be attributed to the rearrangement of propylene and benzene, reaction (17), and isomerization of IPB.

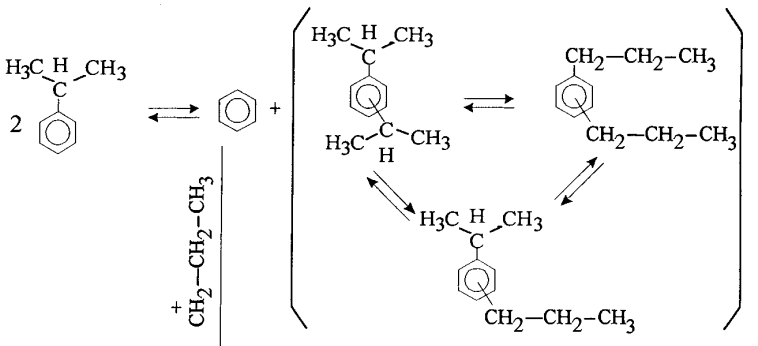

(16)

(17)

At higher reaction temperatures, ca. 200°C, a nearly equal amount of benzene and DIPB and low levels of propylene oligomers were observed. Regarding isomer selectivity, DIPB product is *para* selective at low conversion level (ca. <13%), and *o*-DIPB selectivity is far below the thermodynamic equilibrium composition, which can be attributed to the size exclusion effects of pore openings of ZSM-12.

Tsai et al. [162] compared the catalytic performance of various zeolites on IPB disproportionation as shown in Table 16. It was demonstrated that among zeolite Y, mordenite, ZSM-12 and Beta, the last had

Table 16
Catalytic performances of zeolites in cumene disproportionation

	H–beta[a]	H–Y[a]	H–mordenite[a]	H–ZSM-12[b]
Reaction temperature (°C)	143	220	240	250
Conversion (wt%)	40.1	22.5	14.5	45.1
Coke (g/g_{cat}%)[c]	4.72	4.54	6.62	–
Selectivity (mol/mol)				
Disproportionation	0.98	0.91	0.95	0.90
Benzene/DIPB	1.06	1.16	1.12	1.17
Stability (α)	0.23	0.14	0.31	–
Product Yields (wt%)				
Benzene	13.50	7.74	4.95	15.42
Cumene	59.88	77.53	85.55	54.90
n-Propylbenzene	0.10	0.17	0.14	0.32
DIPB	26.44	13.8	9.22	27.47
Other aromatics	0.08	0.76	0.14	1.89
DIPB isomer distribution				
Para	32.8	30.5	30.5	35.3
Meta	67.2	66.4	65.9	63.9
Ortho	0	3.1	1.2	0.8

[a] Data from [162].
[b] Data from [163].
[c] Coke deposition after 3 h of time-on-stream at the specified reaction conditions.
[d] WHSV: 3.4 g/h g cat, N_2/Cumene=0.19 mol/mol, Time-on-stream: 60 min.

the greatest activity and disproportionation selectivity, as indicated by the lowest benzene-to-DIPB ratio. All zeolites show a ring *positional* isomer distribution similar to that obtained from Friedel–Craft catalysts with the exception of low *o*-DIPB selectivity. Interestingly, compared to other zeolitic catalysts, zeolite Beta has a much better *skeletal* isomer selectivity of DIPB. Tsai et al. [162] proposed a bi-molecular reaction mechanism for IPB disproportionation. A high *skeletal* selectivity would require, (1) a low level of side reactions (e.g., side chain isomerization) to preserve the isopropyl group on the aromatics ring, reaction (16), and (2) inhibition of rearrangement of the ring isopropyl group to form *n*-propylbenzene by cracking-realkylation reaction, reaction (17).

5.3. Stability of cumene disproportionation

In addition to the *skeletal* isomer selectivity, catalytic stability is the other major concern in the development of an industrial IPB disproportionation process. Catalytic stability can be related to the decay constant α by the following empirical equation:

$$X = X_0 t^{-\alpha} \tag{18}$$

where X_0 is the initial conversion at t=0 and X is the measured conversion at time-on-stream t. Typical α values of different zeolites are listed in Table 16. The fact that zeolite Beta has a lower α value compared to the other zeolites indicates that it has a better stability. Tsai et al. [166] have found that the catalytic stability of zeolite Beta can be enhanced either by steam pretreatment or by surface modification with silica deposition. As a result, the α value was reduced from its original value of 0.23 to 0.01 by steam pretreatment, and to 0.08 by silica deposition. Steam pretreatment can reduce coke formation and hence prolong the life of the catalyst. In contrast, surface silica deposition suppresses the formation of coke on the channel pore mouth to avoid the detrimental effects.

Chen et al. [167] reported that catalyst stability can be affected by the type of carrier gas present in the system. They concluded that, in the presence of different carrier gases, catalyst stability increases in the order: CO_2>He>H_2>N_2, with catalyst activity, in the reversed order. Parikh et al. [168] found that the catalytic stability of zeolite Beta during IPB isopropylation can be improved by dealumination, which may be achieved by either steam pretreatment or $(NH_4)_2SiF_6$ treatment. The authors further reported that the catalytic activity remained unchanged after the steam pretreatment but was reduced after treated with $(NH_4)_2SiF_6$.

Table 17
Effects of operating regime on catalytic stability of cumene disproportionation [169]

Operating regime	1	2	3
Reaction temperature (°C)	200	200	150
Reaction pressure (Kg/cm^2)	1	21	21
Phase			
Feed	Vapor	Vapor	Liquid
Product	Vapor	Liquid	Liquid
Catalytic stability	Poor	Excellent	Good

Chang et al. [169] studied the effects of operating conditions on the catalytic stability of mordenite during the IPB disproportionation reaction. The authors employed different operating regimes for feed and product during the calculation using the Clausius–Clapeyron equation (Table 17). It was found that, for mordenite, stable activity is reached only under the operating regimes of feed in vapor phase and product in liquid phase. The operating regime can be altered by proper selection of operating temperature, pressure, carrier gas-to-IPB ratio and types of carrier gas.

In a recent study, Wang et al. [170] observed stable IPB disproportionation over a modified mordenite catalyst which operated under the conditions: temperature, 200–240°C; pressure, 300–400 psig; WHSV, 3–4 h^{-1} with 50% IPB conversion. The typical product distribution was 17 wt% of benzene, 21 wt% of *m*-DIPB and 11 wt% of *p*-DIPB, with benzene-to-DIPB molar ratio of 1.1. No trace of the other *skeletal* isomer formation was found. The catalyst cycle life was estimated at over 6 months.

5.4. Transalkylation of diisopropylbenzene and benzene

Similar to the EB production process, modern IPB production processes also utilize zeolite catalyst [7]. The multi-alkylation side products are recycled to the transalkylation reactor then further react with benzene to form IPB, therefore, enhances the IPB product

yield. In contrast to the EB process, which requires a separate transalkylation reactor, both the transalkylation and isopropylation reaction can be done in the same reactor for the IPB process.

Pradhan et al. [171] concluded that zeolite Beta is more active and more stable than mordenite or La–H–Y during transalkylation of DIPB and benzene. The authors reported that while the stability of zeolite Beta can be enhanced in the liquid phase at 200°C and 25 kg/cm^2, a significant loss in conversion was also observed. They attributed the effects of liquid phase operation to the retardation of coke formation and decrease in the diffusivities of the feed and the product. Moreover, the stability of zeolite Beta can be further improved at the expense of a slight loss in DIPB conversion, by impregnating 0.1 wt% of platinum.

Innes et al. [172] investigated zeolite NH_4-Beta and steam stabilized zeolite Y as catalysts in the transalkylation reaction of benzene and DIPB. The catalyst they used comprised 65% zeolite Beta and 35% alumina. Testing-feed was benzene and DIPB mixture at a molar ratio of 2:1, and the liquid phase reaction was carried out under these conditions: temperature, 138°C; pressure, 35.2 kg/cm^2 and LHSV, 1 h^{-1}. They measured catalyst stability at conversion 35–40% of DIPB and the reaction temperature was raised in order to compensate for catalyst deactivation. During 70 days-on-stream or so, zeolite Beta showed a deactivation rate of 0.19°C/day (Fig. 33), much better than that of steam stabilized Y which has a deactivation rate of 0.44°C/day. It is worth noting that zeolite Beta is also known to be more active than zeolite Omega.

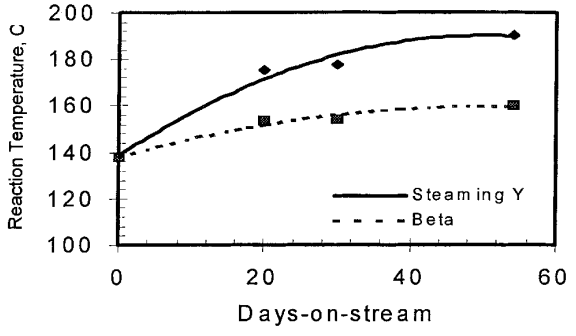

Fig. 33. Comparison of catalytic stability in transalkylation of benzene and DIPB between zeolite Beta and steaming Y zeolite; reaction conditions: feed: benzene/DIPB: 2 wt/wt, DIPB feed: 95% purity with heavy aromatics contaminant, initial reaction temperature: 138°C, pressure: 35.2 kg/cm^2, LHSV: 1 h^{-1}, DIPB conversion: 35–40%, run time: 54 days; data from ref. [172].

6. Cymene production via transalkylation

Cymene is one of the valuable petrochemical intermediates for the production of cresol, which can be used for phenolic resin and plasticisers [173]. It can be produced industrially through toluene alkylation with propylene, a process applying a liquid catalyst which was commercialized by Sumitomo in 1973 [174]. Its cymene product was mainly a *m*- and *p*-cymene mixture, with the *o*-isomer less than 5%. *o*-Cymene isomer is undesirable due to its low oxidation rate and selectivity to *o*-cresol. The *m*- and *p*-cymene mixture was used directly for oxidation to produce *m*- and *p*-cresol mixtures, with a total concentration not less than 99.5%, and 60% *m*-cresol as minimum.

Similar to DIPB, there are six cymene isomers, as listed in Table 2. Among them, the three ring *positional* isomers have very similar physical properties. For example, their boiling points and melting points differ by only a very small amount. Moreover, the physical properties of its *skeletal* isomer, methyl-*n*-propylbenzene (MNPB), are also similar to those of cymene. The industrial production of *p*-cymene is mostly achieved by adsorptive separation from cymene mixtures [52,53]. Selectivity in both their ring *positional* and *skeletal* isomers has a critical impact on cymene separation cost.

Recently, several attempts have been initiated to explore the possibility of using solid acid catalysts in cymene production to phase out the traditional environmentally hazardous Friedel–Craft processes. Zeolites are of course the ideal candidates for such purpose. In their study of toluene propylation over ZSM-5, Dwyer and Klocke [175] found that the selectivity of cymene increases with decreasing reaction temperature, as shown in Fig. 34. A latter investigation by Tsai et al. [162] revealed that, over ZSM-5 zeolite, IPB undergoes dealkylation while *n*-propybenzene undergoes isomerization to form isopropylalkylbenzene with a thermodynamic equilibrium composition [176]. The temperature effects can be attributed to the isomerization of cymene via a dealkylation–alkylation mechanism at high reaction

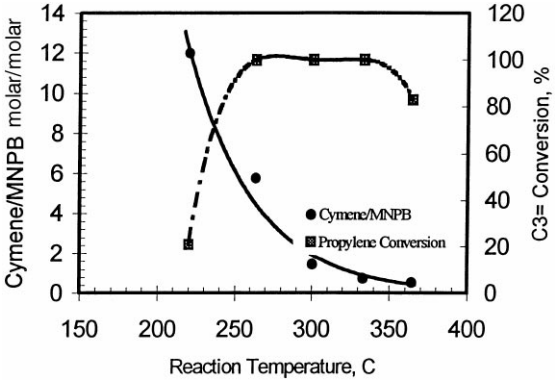

Fig. 34. Plot of cymene selectivity and propylene conversion against reaction temperature in toluene propylation over ZSM-5; reaction conditions: WHSV: 2.3 h^{-1}, propylene/toluene: 26 mol/mol, data from ref. [175].

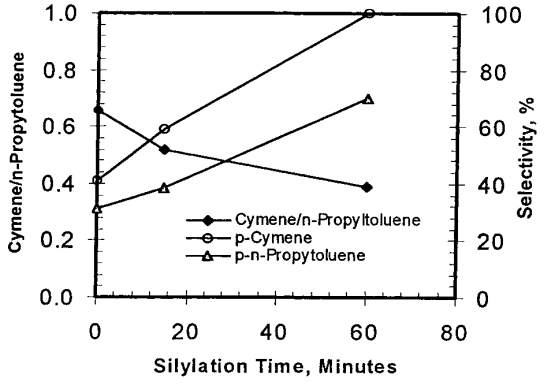

Fig. 35. Effects of extent of silica modification on product selectivity in benzene isopropylation over silica modified ZSM-5; reaction conditions: reaction temperature: 350°C, WHSV: 5.5 h^{-1}, toluene/isopropanol: 4 mol/mol; data from ref. [177].

temperature; the cymene/MNPB ratio of ca. 0.5 is in line with the thermodynamic equilibrium composition.

In the attempt to improve *p*-cymene selectivity, Parikh et al. [177] reported 100% *p*-cymene selectivity over silica modified ZSM-5. Silica modified ZSM-5 zeolite catalysts were more stable than zeolite Beta. As shown in Fig. 35, with increasing extent of silylation, the selectivities of *p*-cymene and MNPB were increased, while cymene yield was decreased. As a result, the cymene/MNPB ratio was reduced to 0.4, far below the equilibrium ratio. Owing to the shape selectivity imposed by the silica modified ZSM-5, only those molecules or product isomers with suitable molecular sizes (such as the *p*-isomers and MNPB) may be formed. However, the challenge to resolve the paradox of enhancing *p*-cymene selectivity while maintaining the cymene selectivity at the same time remains unsolved.

Reddy et al. [178] had compared the performance of large-pore zeolites during IPB isopropylation. Their results are summarized in Table 18. It is clear that the large-pore zeolites all show a much better cymene selectivity against MNPB than ZSM-5. Interestingly, cymene isomers catalyzed by those large-pore zeolites were rich in *meta*-isomer. ZSM-12, which has comparable stability to zeolite Beta, showed slightly higher *p*-cymene selectivity than the others.

Several attempts have been made to explore the potential application in trasalkylation of toluene and IPB, as shown in reaction (19), for cymene production. Bandyopadhyay et al. [179] reported that zeolite Beta has higher activity and cymene yield (ca. 7.9 wt%) compared to both H–Y and H–ZSM-12. As shown in Table 18, transalkylation over zeolite Beta yielded a cymene selectivity among C_{10}^{+} aromatics similar to that given by toluene isopropylation. However, there were high yields of disproportionation products, such as benzene (37.3% yield), DIPB from IPB disproportionation, and xylene (1.8% yield) from toluene disproportionation, as shown in reaction (20). Only a small amount of diisopropyltoluene (DIPT) (1.8% yield) was observed, which has a molecular size larger than the zeolite pore opening of 12-membered oxygen ring [180], and its diffusion is limited.

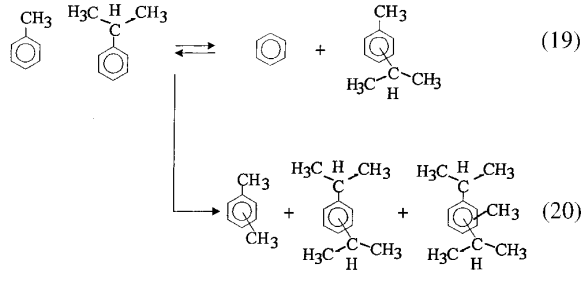

(19)

(20)

7. Future trend and process development

7.1. Para-isomer selectivity with maximum activity retention

The effects of diffusivity on *para* selectivity have been extensively studied for the *p*-xylene production processes. However, little is known regarding the *para*

Table 18
Cymene production processes

Catalyst	ZSM-5[d]	Si/ZSM-5[e]	Beta[f]	Mordenite[f]	HZSM–12[f]	Beta[b,c]
Reaction conditions						
Temperature (°C)	263	300	180	180	180	220
WHSV (h^{-1})	2.3	5.5	4	4	4	4.2
Reaction type			Isopropylation			*Trans*[b]
A_7/isopropanol	26[a]	4	8	8	8	–
Toluene/cumene	–	–	–	–	–	6
Conversion (%)						
Propylene	100	~20	~100	~100	~100	No
Toluene		5.1	11.5	14.2	10.2	7.1
Cumene	No	No	No	No	No	44.9
Total cymene (%)	~4.7	~6.1	16.5	16.2	15.8	7.9
C_{10}^{+} *aromatics selectivity* (%)						
Cymenes	85.2	28	96.6	97.0	94.1	90.6
MNPB	14.8	72	0	0	0	0
DIPT	–	–	2.8	2.3	5.3	1.8
DIPB	–	–	0.6	0.7	0.6	7.6
Cymene/MNPB	5.74	0.39	∞	∞	∞	∞
Cymene distribution (%)						
Para	~20.2	100	30.4	30.3	34.4	29.9
Meta	~79.8	0	64.2	65.1	57.2	64.3
Ortho	~0	0	5.4	4.6	5.7	5.7

[a] Isopropylation reaction by using propylene, expressed for cumene/propylene ratio.
[b] By transalkylation of cumene and toluene.
[c] Ref. [179].
[d] Ref. [175].
[e] Ref. [177], Silylation time was 60 min.
[f] Ref. [178].

selectivity of DEB as well as larger molecules. There are still debates on the main working principles of *para*-isomer selectivity enhancement, e.g., external surface inactivation or/and pore mouth reduction etc. Several techniques have been used. Namba et al. [99,180–182] proposed the cracking reaction of large molecules such as 1,3,5-tri-isopropylbenzene (TIPB) to measure the external surface active sites. Niwa et al. [101,183] pioneered the XPS measurement technique, and recently O'Connor et al. [143] proposed the transformation of 1,2,4-TMB particularly for medium-pore zeolites such as ZSM-5. Diffusivity methods are widely used for measuring zeolite pore openings and structures [184–187]. In addition, Fraissard et al. [188,189] developed the ^{129}Xe NMR method, which can accurately measure the internal void space of zeolites by determining the intercept and the slope of ^{129}Xe chemical shift against various loading pressures of ^{129}Xe-adsorption [190]. Davis et al. [191] proposed the isomerization and alkylation of *m*-DIPB, (by measuring the ratio of 1,3,5- to 1,2,4-TIPB yield) to characterize the effective pore voids in large-pore zeolites with greater than 12-membered oxygen ring. In general, the extent of *para* selectivity enhancement should vary with the type of reaction, type of reactants and products and their molecular sizes; related information on the correlation of diffusivity and *para*-isomer selectivity of alkylbenzenes would be valuable.

At present, *para* selectivity processes have been proven successful only for medium-pore zeolites, especially ZSM-5. Moreover, the enhancement of *para* selectivity is normally achieved at the expense of catalyst activity. For example, a *p*-xylene improvement of 1% is achieved with a conversion loss of 0.4% in precoking selectivation [76], and with a loss of ca.

0.2% by the silica modification method [79]. Surface modified zeolite catalysts required pretreatment procedures mainly to passivate the external surface and/or to reduce diffusivity. It is highly desirable to optimize the pretreatment procedures so that the *para* selectivity can be achieved while maintaining a maximum activity. Potential solutions can be the optimization of preparation methods [79,96,108–112], types of zeolites [117,192], types of binders [79], etc. Some isomorphorously substituted ZSM-5 zeolites have demonstrated the potential for *para* selective reactions [102,193].

7.2. Transalkylation processes

The trend in the petroleum industry worldwide is to produce reformulated gasoline with low benzene (<1.0%) and total aromatics (<20%) contents. As a result, benzene and heavy aromatics would be freed up from reformulated gasoline. Transalkylation processes should be beneficial solutions to this challenge. They can convert heavy aromatics into more favorable products such as xylenes.

More research in heavy aromatics processing is therefore needed. The demanding performance criteria that are related to transalkylation process include:

1. capability in sustaining higher impurity tolerance and less feed specification,
2. capability of processing high A_9 feed percentage,
3. higher throughput capacity,
4. suppression of undesirable A_{10}^+ formation from disproportionation of A_9^+, and
5. flexibility of product modes.

Among them, the first three criteria are of course closely related to zeolite catalyst development.

A_{10}^+ yield usually increases following thermodynamic equilibrium with increasing A_9^+ feed content. The formation of A_{10}^+ in the transalkylation process, which is economically undesirable, can probably be inhibited by applying shape selective catalysis, by fine-tuning zeolite structures to inhibit the formation and/or diffusion out of A_{10} product, or by changing feed compositions, or process integration of transalkylation and dealkylation. The net A_{10}^+ yield can be reduced by adding A_{10} into the feed, such as the operation of TransPlus^{SM} Process. The net yield of A_{10}^+ is the thermodynamic equilibrium yield substrates its concentration in feed.

The proposed dealkylation reaction network can get away thermodynamic control of transalkylation, by which pure heavy aromatics feed are first converted into alkylbenzene, it is then recycled to further transalkylate with the aromatics feed.

7.3. Alkyl group transfer homologous reactions

Since dicarboxic acids of large molecule dialkylbenzenes have shown increasing industrial importance in new engineering plastic materials, there is growing research interest in their production. One particular example is the production of 2,6-NDCA (2,6-napthalene dicarboxic acid) with better physical properties over the traditional dicarboxic acids of single aromatic ring [194]. Its major production schemes involve the production of key intermediate 2,6-DMN (2,6-dimethylnapthalene), which can be obtained by side-chain alkylation of *o*-xylene with base catalysts [195], or alkylation of naphthalene with acid catalysts [196,197]. Recently, Mobil Oil and Kobe Steel jointly developed a new zeolite catalyst for the production of dimethylnaphthalene [198].

Alkylation usually forms side products as in Polyalkyl aromatics. Alkyl group transfer reactions, on the other hand, usually have fewer side products and higher product yields. However, catalysis of alkyl group transfer reactions is very sensitive to molecular size. Most current industrial applications of alkyl group transfer processes (for example, disproportionation and transalkylation) are mainly for methyl and ethylbenzene; fewer are for alkylbenzenes with alkyl groups larger than propyl group or for polynuclear aromatics. Alkylation seems to be more favorable over the alkyl group transfer reaction, especially for systems where the alkyl groups contains larger number carbon atoms.

It has been demonstrated that large-pore zeolites are useful in alkyl group transfer reactions of alkylbenzenes with less than two aromatics rings, while medium-pore zeolites are only good for molecules whose sizes are smaller than IPB. With the recent discovery of new mesoporous materials, it is worthwhile to explore their potential application to extend the current technology of alkyl group transfer reactions to large molecules. Since the number of isomers is proportional to the carbon number of the alkyl group, the enhancement of shape selective catalysis with

better ring *positional* and *skeletal* isomer selectivity will have profound impacts on recovery and production cost. In addition, it is of industrial significance to extend the current shape selective catalysis technology to other alkyl group categories, such as alkenyl group transfer reactions, selective amination, selective oxidation, etc.

Siliceous titanium zeolites, particularly Ti–ZSM-5 (TS-1), were found to be good selective oxidation catalysts [199–201]. The major working principles for this oxidation catalyst were hydrophobicity and oxygen transfer. Selective oxidation of *p*-dialkylbenzene isomers in unseparated mixtures against the other dialkylbenzene isomers is a challenging new technology. If it can be done, oxidation can then be a separation reaction for dialkylbenzene isomers. Among many possibilities, diffusion control of the oxidation rates of different isomers would be worthwhile to study. Since a *p*-dialkylbenzene has a lower oxidation reactivity than an *o*-isomer, diffusion control needs to be very selective for *p*-isomer to prevent the contamination with the dicarboxylic acid of the *o*-isomer.

Several shape selective reactions of heteroatom containing compounds are also of interest. Some examples are the synthesis of *p*-alkylanisols [202], *p*-alkylphenols [203] and *p*-dihalobenzenes [204]. More examples were listed in Chen et al. [23].

7.4. BTX purification

Owing to the enforcement of reformulated gasoline regulations, a large portion of aromatics must be excluded from the gasoline to meet product specification. Thus, a demand for more BTX purification capacities is obvious. Existing aromatic purification technologies are conventional extraction processes [205] or more advanced extractive distillations [206], which are expensive and have limited processing capacity. Many active research programs have been initiated to reduce the requirements of the existing extraction units or even to explore possibility of eliminating the extraction operation. Among those approaches, shape selective catalysis is applied to resolve this new challenge. Among many examples are Mobil's reformate upgrading process, (which has been commercialized to reduce the EB content of the reformate [207]), the use of non-extractive toluene in selective toluene disproportionation reaction [208], etc.

An alternative approach is the direct conversion of alkanes to aromatics [209–211], such as the M-2 Forming [212] and Cyclar^{SM} [213,214] Process. Most of the existing production processes utilize the integration of reforming and extraction processes. The newly developed process might not require an extraction unit and hence is more cost economic in the setup for grass root petrochemical plants. It is expected that future research on direct BTX production will have a substantial impact on the existing BTX production industry.

7.5. Engineering study

Although not being discussed in the present review, alkyl group transfer process technology involves many engineering issues, for example, reactor flow pattern and catalyst loading procedures. In principle, an ideal plug flow pattern is critical for the homogeneity of selectivation pretreatments, such as pre-coking [27] or surface modification by silica deposition. Any channeling flow, which will lead to the formation of thermodynamic equilibrium mixtures to contaminate highly *para* selective product, should be prevented.

Some of the pretreatment procedures involve extreme start-up conditions, including high reaction temperature and low hydrogen-to-aromatics ratio [76,77,141] and sulfiding [140]. Thus, the most original engineering design should allow for a wide range of operating conditions. This concern is particularly critical while processing A_9 feed. Unlike disproportionation of alkylbenzenes, A_9 can undergo dealkylation and re-alkylation with possible excessive heat transfer problems. A comprehensive study on the kinetics of the individual A_9 compounds should be helpful to the design of start-up procedures.

The other engineering related issue concerns the recovery of *p*-xylene. The conventional design for recovery of *p*-xylene is to recover it from thermodynamic equilibrium compositions. It is feasible now to obtain *p*-xylene rich A_8 mixtures either from selective toluene disproportionation processes or by pretreatment by adsorptive separation processes, such as Eluxyl^{SM} (by IFP). Wide ranges of available crystallization techniques, such as falling-film melt crystallization [62,214], are worthwhile evaluating for

integration to enhance *p*-xylene recovery rate from *p*-xylene rich feed. Thus, the optimal recovery scheme for *p*-xylene from *para* rich A_8 mixtures should be searched for. The potential of some earlier innovations on separation can be revisited again for the application with *para*-isomer rich feed [215]. The same strategy used in some of the recent new process designs for the *p*-xylene recovery system may be relevant, but the design for the separation of other dialkylbenzenes has yet to be included.

7.6. Coke formation and catalyst regeneration

Pre-coking treatment has been successfully used in the selectivation of toluene disproportionation. Recently, Fang et al. [105] presented a physical model for pre-coking. Fundamental studies involving location, nature and migration of cokes are important in understanding the effects of pre-coking.

Coking which is controlled by the pore structure and acidity [216] of zeolites is a shape selective reaction [217]. The rate of coking also has pronounced effects on the stability [218–221] and operating cycle length of the catalyst. ZSM-5 zeolite can accommodate coke content beyond ca. 20% and it is located either inside the pore void space or on the external surface [222–224]. Several research studies related to coke formation in alkylbenzene disproportionation [225–228] can be found. Comprehensive studies on the nature of coke [229] and coking mechanism [218] would benefit industrial researchers in searching for effective techniques to extend the cycle length of the process.

Regeneration is the most effective way to reactivate coked catalysts. The regeneration process is normally achieved by controlled burning of coke (which involves a high heat of combustion). The effectiveness of catalyst regeneration is controlled by operating variables such as temperature, pressure, oxygen concentration, etc., by which numerous operating conditions may be set [230,231]. The criteria for a good regeneration procedure are: minimum regeneration time, maximum restoration of catalyst activity and retention of *para* selectivity. Regardless of its practical importance especially in industrial applications, relatively few research studies related to regeneration have been conducted [232,233]. In their recent work, Jong et al. [234] explored the coke burning mechanism by using ^{129}Xe NMR spectroscopy. The overall regeneration performances can be experimentally evaluated by real test reactions. Studies on microstructures such as hydrothermal stability of zeolites, metal migration, etc., can provide fundamental understanding in more detail, which is useful to optimize industrial regeneration procedures.

8. Conclusions

There has been a growing demand for selected aromatics, such as benzene, xylene, etc. In contrast, there is a surplus in the production of other aromatics, such as toluene, *m*-xylene, etc. The surplus is mainly due to the fact that aromatic production is controlled by thermodynamic equilibrium. Alkyl group transfer reactions, such as disproportionation and transalkylation, are useful in interconversion of excess aromatics and hence help balance the market demand and industrial production. This review discussed the prominent reactions for systems ranging from methyl- to propylbenzenes. Recent advances in process development technology and their driving forces, including economics, legislation, and other relevant variables, were also discussed.

Aromatics conversion process technology has advanced rapidly mainly due to recent advancement in zeolite catalysis. In this review, the key criteria for each process development were identified. The transalkylation process converts surplus toluene and A_9^+ into more economically favorable benzene and xylene products. Thus, its key criteria were maximum A_9^+ feed content with increasing impurity tolerance capacity and without the compensation of cycle length. On the other hand, the key criteria for disproportionation of toluene and EB were *para* selectivity with minimum loss in activity and cycle length. The *para*-isomer selectivity was more than 90%. The diisopropylbenzene (DIPB) and cymene production processes have another important criterion in addition to *para*-isomer selectivity and cycle length, that is, *skeletal* isomer selectivity. Since both *m*-diisopropylbenzene (*m*-DIPB) and *p*-diisopropylbenzene (*p*-DIPB) isomers are useful, *para* selectivity is thus not the main criteria of concern. The key criteria of disproportionation of cumene (IPB) include DIPB yield and catalytic stability.

So far, *para* selective processes have been successful only with medium-pore zeolites, especially ZSM-5. Improvement of *para* selectivity is commonly achieved in industrial processes by pre-coking and surface modification by silicon deposition that involves catalyst pretreatment to passivate external surface and to reduce diffusivity. Normally, the *para* selectivity is enhanced with compensation of activity loss. However, the extent of *para*-isomer selectivity enhancement varies with the types of the reaction. The correlation between *para*-isomer selectivity and diffusion rate was established for *p*-xylene production processes. The knowledge needs to be expanded to other systems of alkylaromatics.

The stability of IPB disproportionation catalysts can be improved either by zeolite dealumination, silica deposition, using various types of carrier gas, or employing other different operating regimes. Catalytic activity is stable under the conditions of vapor phase feed and liquid phase product.

Related technologies for xylene recovery were also reviewed. For xylene mixtures with equilibrium composition, *p*-xylene recovery by adsorption techniques is more economical. Alternatively, the crystallization method becomes more economical when the *p*-xylene concentration in xylene mixtures is enhanced. The higher *p*-xylene concentration is either normally achieved by selective toluene disproportionation process or pre-adsorption of equilibrium xylene mixtures. Perspectives of future research in the area of process development have also been discussed and, in some cases, new research directions were proposed.

Acknowledgements

The authors would like to express their gratitude to Dr. N.Y. Chen and Dr. P.B. Venuto for helpful discussions and their valuable suggestions. The kind assistance of W.S. Liaw, C.T. Chiu and Miss S.L. Wang, L.M. Wu, A.C. Tsai during the preparation of this manuscript is also acknowledged.

References

[1] L.F. Hatch, S. Mater, Hydrocarbon Process. 58(1) (1979) 189.
[2] H.A. Wittcoff, The Chemical Industry: Technology and Concepts, Chem Systems Inc., in: Union Chem. Lab., Ind. Tech. Res. Inst., Hsinchu, Taiwan, 12–13 March, 1992.
[3] J.J. Jeanneret, C.D. Low, V. Zukauskas, Hydrocarbon Process. 6 (1994) 43.
[4] J.D. Swift, M.D. Moser, 20th Dewitt Petrochemical Review, 21–23 March 1995.
[5] H.A. Colvin, J. Muse, CHEMTECH 16 (1986) 500.
[6] K. Tanabe, Solid Acids and Bases, Academic Press, New York, 1970.
[7] A. Wood, Chem. Week 17 (1994) 34.
[8] Regulation of Fuels and Fuel Additives, US Federal Legislation 40CFR Part 80, 1994.
[9] R.J. Schmidt, P.L. Bogdan, N.L. Gilsdorf, CHEMTECH N2 (1993) 41.
[10] S.D. Evitt, G. Gong, M.N. Harandi, H. Owen, N.A. Collins, National Petrol. Ref. Assoc., AM-92-55, 1992.
[11] D. Greenaway, PEP Report 182, Stanford Res. Inst., Menlo Park, CA, 1987.
[12] S.M. Leiby, E. Chang, PEP Report 182A, Stanford Res. Inst., Menlo Park, CA, 1997.
[13] S.M. Leiby, PEP Report 209, Stanford Res. Inst., Menlo Park, CA, 1992.
[14] C. Barron, A. Leder, Y. Sakuma, CEH Product Review: Isophthalic Acid, Stanford Res. Inst., Menlo Park, CA, 1995.
[15] A. Mitsutani, K. Maruyama, Chem. Eco. Eng. Rev. V6(9) N77 (1974) 36.
[16] The 1991 World Petrochemical Industry Survey - Aromatics, Parpinelli TECNON srl, Milan, Italy, 1991.
[17] Exxon Estimates for Trade Publications, in National Petrol. Ref. Assoc., Exxon Cheimcals, 1997.
[18] R.G. Harvan, Oil Gas J. 30 (1998) 56.
[19] P.B. Weisz, Pure Appl. Chem. 52 (1980) 2091.
[20] S.M. Csicsery, Pure Appl. Chem. 58 (1986) 841.
[21] W.W. Kaeding, G.C. Barile, M.M. Wu, Catal. Rev.-Sci. Eng. 26(3)(4) (1984) 597.
[22] W.O. Haag, in: D.H. Olson, A. Bisio (Eds.), Proceedings of the Sixth International Zeol. Conference, Butterworths, Surrey, 1984, p. 466.
[23] N.Y. Chen, W.E. Garwood, F.G. Dwyer, Shape Selective Catalysis in Industrial Application, 2nd ed., revised and expanded, Marcel Dekker, New York, 1996.
[24] P.B. Venuto, Micropor. Mater. 2 (1994) 297.
[25] F.R. Ribeiro, F. Alvarez, C. Henriques, F. Lemos, J.M. Lopes, M.F. Ribeiro, J. Mol. Catal. A 96 (1995) 245.
[26] C.B. Khouw, M.E. Davis, in: M.E. Davis, S.L. Suib (Eds.), ACS Symp. Ser. 517 (1993) 517.
[27] F. Gorra, L.L. Breckenridge, W.M. Guy, R.A. Sailor, Oil Gas J. 12 (1992) 60.
[28] H.G. Lesnoy, Hydroc. Asia, Nov/Dec (1993) 16.
[29] Europ. Chem. News, 11 (1995) 24.
[30] J.A. Johnson, C.A. Roeseler, T.J. Stoodt, 22nd Annual DeWitt Petrochemical Review, Houston, TX, 18–20 March 1997.
[31] I. Wang, C.L. Ay, B.J. Lee, M.H. Chen, Proceedings of the Ninth International Congress on Catalysis, Calgary, 1988, p. 324.

[32] T. Ponder, Hydroc. Process. (1979) 141.
[33] J.H. D'auria, T.J. Stoodt, Hart's fuel technology and management, (1997) 35.
[34] J.R. Mowry, in: R.A. Meyers (Ed.), Handbook of Petroleum Refining Processes, Section 10–10, McGraw-Hill, New York, 1986.
[35] T.C. Tsai, D.S. Huang, C.M. Lin, C.T. Chiu, J.W. Kao, C.S. Ku, K.Y. Tsai, J. Beech, T. Kinn, S. Mizrahi, N. Rouleau, A. Sapre, H.J. Wang, 2nd Joint China/US Chemical Engineering Conference, Beijing, 19–22 May 1997.
[36] L. Farnos, BTX Intermediates and Derivatives Conference, Singapore, 19–20 June 1997.
[37] J. Beech, R. Cinimi, N. Rouleau, T.C. Tsai, The Aromatics, V51 (1999), to be published.
[38] Mobil TransPlus Process Brochure, Mobil Technology Company.
[39] W.M. Meier, D.H. Olson, Atlas of Zeolite Structure Types, 3rd revised ed., Int. Zeolite Assoc., Butterworth-Heinemann, Boston, MA, 1992.
[40] T.E. Whyte, R.A. Dalla Betta, Catal. Rev.-Sci. Eng. 24 (1982) 567.
[41] V.J. Frilette, W.O. Haag, R.M. Lago, J. Catal. 67 (1981) 218.
[42] D.H. Olson, W.O. Haag, R.M. Lago, J. Catal. 61 (1980) 390.
[43] I. Wang, T.J. Chen, K.J. Chao, T.C. Tsai, J. Catal. 60 (1979) 140.
[44] Chem. Eng. News, 30 (1997) 32.
[45] M.E. Leonowicz, J.A. Lawton, S.L. Lawton, R.K. Rubin, Science 264 (1994) 1910.
[46] M.E. Davis, C. Montes, J.M. Garces, Am. Chem. Soc. Symp. Ser. 398 (1989) 291.
[47] C.T. Kresge, M.E. Leonowicz, W.J. Roth, J.C. Virtuli, J.S. Beck, Nature 359 (1992) 710.
[48] J.S. Beck, J.C. Virtuli, W.J. Roth, M.E. Leonowicz, C.T. Kresge, K.D. Schmitt, C.T.-W. Chu, J. Am. Chem. Soc. 114 (1992) 10834.
[49] ECN, November 21 (1994) 25–26.
[50] M.T. Janes, 16th 1995 Dewitt Petrochemical Review, 19–21 March 1991.
[51] S.L. Wang, Simulation results using PROII package (Sim Science), personal communication.
[52] J.R. Mowry, in: R.A. Meyers (Ed.), Handbook of Petroleum Refining Processes, Section 8-8, McGraw-Hill, New York, 1986.
[53] J.A. Johnson, R.G. Kabza, I. Chem.E. Symp. Ser. 118, p. 35.
[54] L. Mank, A. Hennico, J.L. Gendler, 20th 1995 Dewitt Petrochemical Review, 21–23 March 1995.
[55] G. Hotier, L. Mank, P. Renard, E.Y. Bourg, Ref. LNG and Petrochem Asia 94, Singapore, 1994.
[56] G. Hotier, P. Mikitenko, S.R. Macpherson, WO 9 620 907 (1996).
[57] P. Mikitenko, G. Hotier, EP 7 65 850 (1997).
[58] S.R. Macpherson, P. Mikitenko, WO 9 622 262 (1996).
[59] J.W. Ko, Personal communication.
[60] E.F. Machell, J.E. Wylie, R.B. Thompson, US Patent 3 662 013 (1972).
[61] M.A. Garazi, P.M. Haure, D.G. Daniel, Ind. Eng. Chem. Design Dev. V23(4) (1984) 847.
[62] N.P. Wynn, CEP V88(3) (1992) 52.
[63] A. Chauvel, G. Lefevre, Petrochemical Processes Technical and Economic Characteristics, Editions Technip, Paris, 1989, pp. 255–300.
[64] S. Rajagopal, K.M. Ng, J.M. Douglas, AIChE V37(3) (1991) 437.
[65] D.B. Broughton, R.W. Neuzil, J.M. Pharis, C.S. Brearley, The Separation of *p*-xylene from C_8 hydrocarbon mixtures by the parex process, Third Joint Annual Meeting, AICHE and Puerti Rican IChE, Puerto Rico, 17–20 May, 1970.
[66] J. Swift, D.C. Adams, A.J. Craglione, P.B. Maise, Hydroc. Asia, (1998) 42.
[67] M.S. Belenkil, G.P. Pavlov, N.V. Ulitskaya, SO Patent 192 190 (1964).
[68] A.P. Lien, D.A. McCaulay, J. Am. Chem. Soc. 75 (1953) 2107.
[69] 1977 Petrochemical Handbook, Hydro. Process. 56(11) (1977) 132.
[70] G.M. Wells, Handbook of Petrochemicals and Processes, Gower Press, Vermont, 1991.
[71] W.O. Haag, N.Y. Chen, in: L.L. Hegedus (Ed.), Catalyst Design, Progress and Prospectives, Wiley, New York, 1987, p. 193.
[72] Mobil TDP-3 Brochure, Mobil Technology Company.
[73] S. Han, D.S. Shihabi, R.P.L. Absil, Y.Y. Huang, S.M. Leiby, D.O. Marler, J.P. McWilliams, Oil Gas J. 21 (1989) 83.
[74] K.P. Menard, Oil Gas J. 16 (1987) 46.
[75] Sud Chemi Brochure, Sud Chemi AG.
[76] W.O. Haag, D.H. Olson, US Patent 4 117 026 (1978).
[77] W.O. Haag, D.H. Olson, US Patent 4 097 543 (1978).
[78] A.D. Fremuth, W.D. Eccli, J.L. Pickering, WO 95/26947 (1995).
[79] C.D. Chang, S. Shihabi, US Patent 5 243 117 (1993).
[80] T. Yashima, H. Ahmad, K. Yamazaki, M. Katsuta, N. Hara, J. Catal. 16 (1970) 273.
[81] N.Y. Chen, US Patent 4 002 697 (1977).
[82] N.Y. Chen, W.W. Kaeding, F.G. Dwyer, J. Am. Chem. Soc. 101 (1979) 6783.
[83] W.W. Kaeding, L.B. Young, B. Weinstein, S.B. Butter, J. Catal. 67 (1981) 159.
[84] W.W. Kaeding, C. Chu, L.B. Young, S.A. Butter, J. Catal. 69 (1981) 392.
[85] W.W. Kaeding, L.B. Young, C.C. Chu, J. Catal. 89 (1984) 267.
[86] L.B. Young, S.A. Butter, W.W. Kaeding, J. Catal. 76 (1982) 418.
[87] I. Wang, C.L. Ay, B.J. Lee, M.H. Chen, Appl. Catal. 54 (1989) 257.
[88] N.R. Meshram, J. Chem. Tech. Biotechnol. 37 (1987) 111.
[89] C.V. Hidalgo, M. Kato, T. Hattori, M. Niwa, Y. Murakami, Zeolites V4 (1984) 175.
[90] P. Tynjala, T.T. Pakkanen, J. Mol. Catal. A 122 (1997) 159.
[91] D.H. Olson, W.O. Haag, Catalytic materials relationship between structure and reactivity, ACS Symp. Ser. 248 (1984) 275.
[92] S.M. Csicsery, Zeolites 4 (1984) 202.
[93] N.Y. Chen, in: J.W. Ward (Ed.), Stud. Surf. Sci. Catal., vol. 38, Elsevier Amsterdam, 1988, p. 153.

[94] J. Wei, J. Catal. 76 (1982) 433.
[95] D. Theodorou, J. Wei, J. Catal. 83 (1983) 205.
[96] Y.S. Bhat, J. Das, K.V. Rao, A.B. Halgeri, J. Catal. 159 (1996) 368.
[97] D. Fraenkel, Ind. Eng. Chem. Res. 29 (1990) 1814.
[98] T. Hibino, M. Niwa, Y. Murakami, J. Catal. 12 (1991) 551.
[99] J.H. Kim, A. Ishida, M. Okajima, M. Niwa, J. Catal. 161 (1996) 387.
[100] J.H. Kim, T. Kunieda, M. Niwa, J. Catal. 173 (1998) 433.
[101] M. Niwa, S. Kato, T. Hattori, Y. Murakami, J. Chem. Soc., Faraday Trans. 1(80) (1984) 3135.
[102] J.H. Kim, S. Namba, T. Yashima, Zeolites 11 (1991) 59.
[103] J.H. Kim, S. Namba, T. Yashima, Appl. Catal. 83 (1992) 51.
[104] W.H. Chen, S.J. Jong, A. Pradhan, T.Y. Lee, I. Wang, T.C. Tsai, S.B. Liu, J. Chin. Chem. Soc. 43 (1996) 305.
[105] L.Y. Fang, S.B. Liu, I. Wang, (1998), submitted for publication.
[106] A.G. Ashton, S. Batmanian, J. Dwyer, I.S. Elliott, F.R. Fitch, J. Mol. Catal. 34 (1986) 73.
[107] P.G. Rodewald, US Patent 4 060 568 (1977).
[108] P.G. Rodewald, US Patent 4 090 981 (1978).
[109] P.G. Rodewald, US Patent 4 0127 616 (1978).
[110] P.G. Rodewald, US Patent 4 145 315 (1979).
[111] R.P.L. Absil, S. Han, D.O. Marler, D.S. Shihabi, US Patent 4 851 604 (1989).
[112] R.P.L. Absil, D.S. Shihabi, D.O. Marler, C.D. Chang, D.M. Mitko, US Patent 5 173 461 (1992).
[113] P.G. Rodewald, US Patent 4 477 583 (1984).
[114] P.G. Rodewald, US Patent 4 465 886 (1984).
[115] C.D. Chang, C.T.-H. Chu, T.F. Degnan Jr., P.G. Rodewald, D.S. Shihabi, WO 96/03360 (1996).
[116] J.S. Beck, D.H. Olson, S.B. McCullen, US Patent 5 367 099 (1994).
[117] J.S. Beck, R.M. Dessau, WO 95/31421 (1995).
[118] C.D. Chang, P.C. Rodenwald, US Patent 5 349 113 (1994).
[119] C.C. Chu, US Patent 4 548 914 (1985).
[120] R.M. Lago, D.O. Marler, S.B. McCullen, US Patent 5 349 114 (1994).
[121] D. Rotman, Chemical Week 30 (1995) 18.
[122] I. Wang, B.J. Lee, M.H. Chen, US Patent 4 950 835 (1990).
[123] C.D. Chang, P.G. Rodewald, US Patent 5 516 736 (1996).
[124] M. Niwa, Y. Kawashima, Y. Murakami, J. Chem. Soc., Faraday Trans. I 81 (1985) 2757.
[125] I. Wang, T.C. Tsai, S.T. Huang, Ind. Eng. Chem. Res. 29 (1990) 2005.
[126] K.J. Chao, L.J. Leu, Zeolites 9 (1989) 193.
[127] T.C. Tsai, I. Wang, J. Catal. 133 (1992) 136.
[128] T.C. Tsai, unpublished data.
[129] J. Das, Y.S. Bhat, A.B. Halgeri, Catal. Lett. 23 (1994) 161.
[130] N.R. Meshram, S.B. Kulkarni, P. Ratnasamy, J. Chem. Tech. Biotechnol. A34 (1984) 119.
[131] R.F. Sulivan, C.J. Egan, G.E. Langlois, R.P. Sieg, J. Am. Soc. Chem. 83 (1961) 1156.
[132] N.Y. Chen, W.J. Reagan, J. Catal. 59 (1979) 123.
[133] S.C. Tsai, MS Dissertation, National Tsing Hua University, Hsinchu, Taiwan, 1998.
[134] T.C. Tsai, H.C. Hu, F.S. Jeng, K.Y. Tsai, Oil Gas J. 13 (1994) 115.
[135] J. Das, Y.S. Bhat, A.I. Bhardwaj, A.B. Halgeri, Appl. Catal. A 116 (1994) 71.
[136] R.P. Absil, S. Han, D.O. Marler, J.C. Vartuli, P. Varghese, US Patent 5 030 787 (1991).
[137] J.C. Wu, L.J. Leu, Appl. Catal. 7 (1983) 283.
[138] E.S. Shamshoum, A.K. Ghosh, J.R. Butler, US Patent 5 475 180 (1995).
[139] J.A. Brennan, R.A. Morrison, US Patent 4 078 990 (1978).
[140] J.S. Buchanan, A.W. Chester, S.L.A. Fung, T.F. Kinn, S. Mizrahi, WO 96/24568 (1996).
[141] E.S. Shamshoum, A.K. Ghosh, T.R. Schuler, US Patent 5 387 732 (1995).
[142] S.M. Csicsery, J. Catal. 19 (1970) 394.
[143] H.P. Roger, K.P. Moller, C.T. O'Connor, Microp. Mater. 8 (1997) 151.
[144] J.R. Chang, F.C. Sheu, Y.M. Cheng, J.C. Wu, Appl. Catal. 33 (1987) 39.
[145] I. Wang, T.C. Tsai, C.L. Aye, Stud. Surf. Sci. Catal. V75 (1993) 1673.
[146] H.G. Karge, J. Ladebeck, Z. Sarbak, K. Hatada, Zeolites 2 (1982) 94.
[147] T.C. Tsai, Ph.D. Dissertation, National Tsing Hua University, Hsinchu, Taiwan, 1991.
[148] W.W. Kaeding, J. Catal. 95 (1985) 512.
[149] Y.S. Bhat, J. Das, A.B. Halgeri, Chemical Weekly 20 (1996) 163.
[150] Technical Bulletin, Hercules Corp., Wilmington, Del., 1989.
[151] H.W. Scheeline, PEP Rep. 79, Stanford Res. Inst., Menlo Park, CA, 1972.
[152] H.W. Scheeline, J.I. Pons, PEP Rep. 79A, Stanford Res. Inst., Menlo Park, CA, 1979.
[153] C.F. Hobbs, D.E. McCakins, Org. Prep. Proced. Int. 4 (1972) 261.
[154] A. D'Onofrio, J. Appl. Polym. Sci. 8 (1964) 521.
[155] L. Bostian, US Patent 3 340 229 (1967).
[156] F. Schnefer, US Patent 4 429 096 (1984).
[157] J. Rinde, H. Newey, US Patent 4 252 936 (1981).
[158] P. Sykes, A Guide to Mechanism in Organic Chemistry, Longman, New York, 1970, p. 260.
[159] R.B. Egbert, R. Landau, A. Saffer, German Patent 1 268 125 (1968).
[160] G.L. Hervert, US Patent 3 763 259 (1973).
[161] R.M. Suggitt, US Patent 3 780 123 (1973).
[162] W.W. Kaeding, J. Catal. 120 (1989) 409.
[163] W.W. Kaeding, Eur. Patent Appl. EP 148 584 (1985).
[164] W.W. Kaeding, Eur. Patent Appl. EP 149 508 (1985).
[165] T.C. Tsai, C.L. Ay, I. Wang, Appl. Catal. 77 (1991) 199.
[166] T.C. Tsai, I. Wang, Appl. Catal. 77 (1991) 209.
[167] W.H. Chen, A. Pradhan, S.J. Jong, T.Y. Lee, I. Wang, T.C. Tsai, S.B. Liu, J. Catal. 163 (1996) 436.
[168] P.A. Parikh, N. Subrahmanyam, Y.S. Bhat, A.B. Halgeri, J. Mol. Catal. 88 (1994) 85.
[169] S.L. Chang, Master Dissertation, National Tsing Hua University, Hsinchu, Taiwan, 1997.
[170] I. Wang, 1998, unpublished data.

[171] A.R. Pradhan, B.S. Rao, Appl. Catal. A 106 (1993) 143.
[172] R.A. Innes, S.I. Zones, G.J. Nacamuli, US Patent 4 891 458 (1990).
[173] W.J. Welstead Jr., , Kirk-Othmer Encyclopedia Chem. Tech. 22 (1978) 709.
[174] K. Ito, Hydrocarbon Process. 52(8) (1973) 89.
[175] F.G. Dwyer, D.J. Klocke, US Patent 4 049 737 (1977).
[176] T.C. Tsai, I. Wang, J. Catal. 133 (1992) 136.
[177] P.A. Parikh, N. Subrahmanyam, Y.S. Bhat, A.B. Halgeri, Appl. Catal. A 90 (1992) 1.
[178] K.S.N. Reddy, B.S. Rao, V.P. Shiralkar, Appl. Catal. A 121 (1995) 191.
[179] R. Bandyopadhyay, R.S. Singh, R.A. Shaikh, Appl. Catal. A 135 (1996) 249.
[180] S. Namba, S. Nakanishi, T. Yashima, J. Catal. 88 (1984) 505.
[181] S. Namba, A. Inaka, T. Yashima, Zeolites 6 (1986) 107.
[182] T. Hibino, M. Niwa, Y. Murakami, Zeolites 13 (1993) 518.
[183] Y. Murakami, Stud. Surf. Sci. Catal. 44 (1989) 177.
[184] D.H. Olson, G.T. Kokotailo, S.L. Lawton, J. Phys. Chem. 85 (1981) 2238.
[185] P. Wu, A. Debebe, Y.H. Ma, Zeolites 3 (1983) 118.
[186] R. Le Van Mao, V. Ragaini, G. Leofanti, R. Fois, J. Catal. 81 (1983) 418.
[187] H.J. Doelle, J. Heering, L. Riekert, L. Marosi, J. Catal. 71 (1981) 27.
[188] I. Demarquay, J. Fraissard, Chem. Phys. Lett. 136, N(3,4) (1987) 314.
[189] R. Benslama, J. Frissard, A. Albizane, F. Fajula, F. Figueras, Zeolites 8 (1988) 196.
[190] S.B. Liu, J.F. Wu, L.J. Ma, T.C. Tsai, I. Wang, J. Catal. 132 (1991) 432.
[191] M.H. Kim, C.Y. Chen, M.E. Davis, in: M.E. Davis, S.L. Suib (Eds.), ACS Symp. Ser. 517 (1993) 222.
[192] D.O. Marler, US Patent 5 329 059 (1994).
[193] A.B. Halgeri, Y.B. Bhat, S. Unnikrishnan, T.S.R. Rao, in: ACS Symposium on Alkylation, Aromatization, Oligomerization and Isomerization of Short Chain Hydrocarbons over Heterogeneous Catalysis, Division of Petroleum Chemistry, NY, 25–30 August 1991.
[194] C. Song, H.H. Schobert, Fuel Process. Techol. 34 (1993) 157.
[195] G.G. Eberhardt, H.J. Peterson, J. Org. Chem. 30 (1965) 82.
[196] P. Moreau, A. Finiels, P. Geneste, J. Solofo, J. Catal. 136 (1992) 487.
[197] C. Song, S. Kirby, Microp. Mater. 2 (1994) 467.
[198] A. Wood, R. Westervelt, Chemical Week 9 (1996) 27.
[199] B. Nortari, Stud. Surf. Sci. Catal. 37 (1987) 413.
[200] J.S. Reedy, S. Sivasankar, P. Ratnasamy, J. Mol. Catal. 70 (1991) 335.
[201] A. Corma, M.A. Camblor, P. Etsteve, A. Martinez, J. Perez-Pariente, J. Catal. 145 (1994) 145.
[202] L.B. Young, US Patent 4 371 714 (1983).
[203] Toray Industries, Japan Patent 61-050 933 (1986).
[204] Asahi Chem, Japan Patent 59-219 241 (1984).
[205] J.Jeanneret, Upgrading BTX Extraction Units, Technical Brochure, UOP Des Plaines, IL, 1993.
[206] J.C. Gentry, C.S. Kumur, Hydrocarbon Process. (1998) 69.
[207] C.M. Sorensen, M.N. Harandi, A. Sapre, D.G. Freyman, AM97-48, San Antonio, 16 (1977).
[208] G.L. Nacamuli, R.A. Innes, EP 704 416 A1 (1996).
[209] C.D. Gosling, R.S. Haizmann, US Patent 5 472 593 (1995).
[210] K.J. Del Rossi, D.J. Dovedytis, D.J. Esteves, M.N. Harandi, A. Huss Jr., WO 94/08921 (1993).
[211] A.B. Bailey, US Patent 4 053 388 (1977).
[212] N.Y. Chen, T.Y. Yan, Ind. Eng. Chem. Process Design Dev. 25 (1986) 151.
[213] B.S. Kawak, W.M.H. Sachtler, W.O. Haag, J. Catal. 149 (1994) 465.
[214] 1995 Petrochemical Handbook, Hydro. Process. (1995) 93.
[215] C.Y. Cheng, S.W. Cheng, US Patent 4 650 507 (1987).
[216] G.D. McLellan, R.F. Howe, J. Catal. 99 (1986) 486.
[217] L.D. Rollman, D.E. Walsh, J. Catal. 56 (1979) 139.
[218] M. Guisnet, P. Magnoux, Appl. Catal. 54 (1989) 1.
[219] S. Bhatia, J. Beltramini, D.D. Lo, Catal. Rev.-Sci. Eng. 31(4) (1989–90) 431.
[220] W.A. Groten, B.W. Wojciechowski, J. Catal. 122 (1990) 362.
[221] G.F. Froment, J. De Meyer, E.G. Derouane, J. Catal. 124 (1990) 391.
[222] D.M. Bibby, N.B. Milestone, J.E. Patterson, L.P. Aldridge, J. Catal. 97 (1986) 493.
[223] T. Behrsing, H. Jaeger, J.V. Sanders, Appl. Catal. 54 (1989) 289.
[224] A. Pradhan, S.J. Jong, W.H. Chen, J.F. Wu, T.C. Tsai, S.B. Liu, Appl. Catal. A 159 (1997) 187.
[225] P. Magnoux, C. Canaff, F. Machado, M. Guisnet, J. Catal. 134 (1992) 286.
[226] C.C. Lin, S.W. Park, W.J. Hatcher Jr., , Ind. Eng. Chem. Process Des. Dev. 22 (1983) 609.
[227] S.B. Liu, S. Prasad, J.F. Wu, L.J. Ma, T.C. Yang, J.T. Chiou, J.Y. Chang, T.C. Tsai, J. Catal. 142 (1993) 664.
[228] F. Niu, H. Hofmann, Appl. Catal. A 128 (1995) 107.
[229] H.G. Karge, in: E.M. Flanigen, J.C. Jansen (Eds.), Stud. Surf. Sci. Catal. vol. 58, Chapter 14, Elsevier, Amsterdam, 1991, p. 531.
[230] Y. Chang, D.D. Perlmutter, AIChE J. 33(6) (1987) 940.
[231] F.A. Smith, US Patent 4 480 144 (1984).
[232] P. Magnoux, M. Guisnet, Appl. Catal. 38 (1988) 341.
[233] D.R. Acharya, M.R. Ghassemi, R. Hughes, Appl. Catal. 58 (1990) 53.
[234] S.J. Jong, A.R. Pradhan, J.F. Wu, T.C. Tsai, S.B. Liu, J. Catal. 174 (1998) 210.